NASA CONTRACTOR REPORT

NASA CR-651

NASA CR-651

GPO PRICE $ _____

CFSTI PRICE(S) $ 2.50

Hard copy (HC) _____

Microfiche (MF) .25

ff 653 July 65

FACILITY FORM 602

N67 13180
(ACCESSION NUMBER)

74
(PAGES)

CR-651
(NASA CR OR TMX OR AD NUMBER)

CRYOGENIC LIQUID EXPERIMENTS IN ORBIT

VOLUME I: LIQUID SETTLING AND INTERFACE DYNAMICS

by T. E. Bowman

Prepared by
MARTIN MARIETTA CORPORATION
Denver, Colo.
for George C. Marshall Space Flight Center

NATIONAL AERONAUTICS AND SPACE ADMINISTRATION • WASHINGTON, D. C. • DECEMBER 1966

NASA CR-651

CRYOGENIC LIQUID EXPERIMENTS IN ORBIT

VOLUME I: LIQUID SETTLING AND INTERFACE DYNAMICS

By T. E. Bowman

Distribution of this report is provided in the interest of information exchange. Responsibility for the contents resides in the author or organization that prepared it.

Prepared under Contract No. NAS 8-11328 by
MARTIN MARIETTA CORPORATION
Denver, Colo.

for George C. Marshall Space Flight Center

NATIONAL AERONAUTICS AND SPACE ADMINISTRATION

For sale by the Clearinghouse for Federal Scientific and Technical Information
Springfield, Virginia 22151 – Price $2.50

FOREWORD

This report was prepared by the Martin Company under Contract NAS8-11328, Cryogenic Liquid Experiments in Orbit, for the George C. Marshall Space Flight Center of the National Aeronautics and Space Administration. The work was administered under the technical direction of the Propulsion and Vehicle Engineering Laboratory, George C. Marshall Space Flight Center, with Gordon Platt acting as project manager.

CONTENTS

		Page
Foreword		iii
Contents		v
Summary		ix
Symbols		xi and xii
I.	Liquid Settling and Interface Dynamics	1
	A. Introduction	1
	1. Surface Shape	2
	2. Surface Dynamics	3
	3. Liquid Flow	4
	B. Analysis	5
	1. Dynamic Equations	6
	2. The Eigenvalue Problem and Stability Considerations	10
	3. Response to an Applied Acceleration	21
	4. The Axisymmetric Case	23
	5. The Effect of Offaxis Accelerations	28
	C. Experiments	34
	1. The Original Investigation: Settling Bond Numbers from 0 to 400	34
	2. Extension to the Range of Settling Bond Numbers from 400 to 2000	45
	3. Investigation of the Effect of Offaxis Accelerations	50
	D. Discussion and Conclusions	56
	1. Approximations in the Analysis	56
	2. Contact Angle	57
	3. Conclusions	58

II. Recommendations 60

III. References . . . . . 61 thru 64

Figure

I-1 System of Interest 5

I-2 Degree of Instability of Axisymmetric Modes, $h/R \geq 1.0$ 15

I-3 Degree of Instability of Axisymmetric Modes, $h/R = 0.5$ 16

I-4 Degree of Instability of Axisymmetric Modes, $h/R = 0.2$ 17

I-5 Degree of Instability of Axisymmetric Modes, $h/R = 0.1$ 18

I-6 Axisymmetric Interface Shape 19

I-7 Axisymmetric Modes, Cross Section thru Axis . . 20

I-8 $B_{R_o} = 1000$, $B_R = -30$ 25

I-9 $B_{R_o} = 1000$, $B_R = -200$ 25

I-10 $B_{R_o} = 1000$, $B_R = -600$ 25

I-11 $B_{R_o} = 1000$, $B_R = -1000$ 25

I-12 $B_{R_o} = 0$, $B_R = -10$ 26

I-13 $B_{R_o} = 0$, $B_R = -100$ 26

I-14 $B_{R_o} = 0$, $B_R = -2500$ 26

I-15 $B_{R_o} = 20$, $B_R = -100$ 26

I-16 $B_{R_o} = 20$, $B_R = -1000$ 27

I-17 Analytical Results, $\alpha_o = 0$ deg 30

I-18	Analytical Results, α_o = 1 deg	31
I-19	Analytical Results, α_o = 10 deg	32
I-20	Experimental Apparatus	35
I-21	General Classification of the Observed Flows . .	37
I-22	Additional Features of the Central Flow Observed in Certain Regime 5 Flows	38
I-23	7.6- and 9.5-cm Cylinders at 0.016 g (Freon TF).	41
I-24	2.3-, 4.7-, 13.2-, and 15.2-cm Cylinders at 0.016 g (Freon TF)	42
I-25	29.2-cm Cylinder at 0.016 g (Freon TF)	43
I-26	18-in. Test Specimen	46
I-27	B_R = -1200	47
I-28	B_R = -1700 (1.5 sec)	48
I-29	Experimental Apparatus	51
I-30	Experimental Results	52
I-31	Influence of 1-deg Acceleration Misalignment on the Flow	55

SUMMARY

Many propellant storage and handling problems encountered by the Saturn V/S-IVB, and other future vehicles can be solved only by orbiting experiments. Because of the complexities and cost of such an operation, it is necessary to design the experiments carefully. This project was planned to clarify certain aspects of fluid mechanics pertaining to low-gravity conditions and thus support the experimental design effort.

The results of an investigation of liquid settling and interface dynamics, one of the four areas of investigation included in the overall program, are presented in this volume. The other areas of investigation, which are reported in Volume II, were concerned with nucleate boiling, liquid venting, and the general behavior of bubbles under low gravity.

Liquid Settling and Interface Dynamics - The dynamic response of a liquid surface to sudden changes in axial or offaxis acceleration was investigated both analytically and experimentally. The analysis was based on potential flow equations, linearized about a plane. A solution was obtained in the form of a Fourier-Bessel series, and was evaluated for a number of cases of acceleration reversal. Various combinations of high and low initial and final accelerations were plotted. The experiments, performed in a 75-ft drop tower, consisted of accelerating test specimens downward, relative to free fall, for 2.1 sec. Experiments were performed at settling Bond numbers $(\rho a R^2/\sigma)$ from 0 to 1730, with nearly flat initial surfaces in every case.

Good qualitative agreement was obtained between the results of the analytical and experimental portions of the program. The analysis of the initial interface dynamics complements the experiments by providing an understanding of the reasons why the experimentally observed settling flows develop as they do, and the experiments in turn complement the analysis by providing an understanding of the detailed characteristics of the flow that result from the initial surface deformations.

The experimental results provide a valid representation of what would occur in an actual space vehicle tank for the same initial conditions and boundary conditions. Both the analysis and the experiments show that primary aspects of the settling flow are scaled by Bond number. The analysis further shows that these same flow characteristics should be essentially independent of contact angle.

Both the analysis and the experiments also showed that the axisymmetric case is in some ways singular. Very slightly off-axis accelerations can result in almost all of the liquid moving up one side of the container.

Engineering questions relating to flow velocities and the total amount of time required for liquid to move from one end of a tank to the other and come to rest again still cannot be answered. Drop-tower experiments have not been able to adequately investigate these long-duration effects. The analysis does not really even consider flow characteristics, much less the fluid behavior once the flow has reached the end of the tank, and also does not take account of the effects of viscosity and contact angle variations, both of which are important in considering flow velocities.

SYMBOLS

a	Acceleration
$B_{\alpha R}$	$\frac{(\rho_1 - \rho_2)aR^2}{\sigma} \cos \alpha$ (a modified Bond number)
D	Vessel diameter
h	Fluid depth (see Fig. 1)
I	Modified Bessel function of the first kind
J	Bessel function of the first kind
k	Wave number
L	Vessel length
	Wave length
p	Pressure
r	Radial coordinate
R	Vessel radius
t	Time
z	Vertical coordinate
α	Direction of acceleration
β	Modified capillary constant, $\frac{(\rho_1 - \rho_2)a}{\sigma} \cos \alpha$
γ	Contact angle

η	Surface displacement (see Fig. 1)
θ	Angular coordinate
ρ	Fluid density
σ	Surface tension
φ	Velocity potential
ω	Wave frequency (see Eq [13]
Bond Number	Dimensionless ratio of inertia forces to surface tension forces, $\frac{(\rho_1 - \rho_2)aR^2}{\sigma}$

Subscripts

0	Conditions existing at t = 0
1	Properties of lower fluid (see Fig. 1)
2	Properties of upper fluid (see Fig. 1)
m,n	Indices

I. LIQUID SETTLING AND INTERFACE DYNAMICS

A. INTRODUCTION

Space vehicles typically perform missions that involve a number of reversals in the direction of the vehicle's acceleration. At injection into orbit, for example, a high acceleration is replaced by a small deceleration (from the thin atmosphere that exists even at orbital altitudes) as the main engines shut off. During orbit, small ullaging motors might be fired, replacing the deceleration with a small acceleration to move liquid propellants to the rear portions of their tanks before venting the tanks or restarting the main engine.

If liquid in a vehicle is at rest before one of these changes in acceleration, its free surface shape is determined by the acceleration of the vehicle, the tank dimensions, surface tension, and the densities of the liquid and gases. Following a change in vehicle acceleration, this surface is no longer in equilibrium. It therefore moves in response to the new acceleration, assuming a complex wave shape somewhat in the fashion of a membrane that has been plucked. If all the waves are stable, the liquid surface oscillates about a new equilibrium position. If any wave is unstable, however, flow results as the liquid and gas seek a new equilibrium orientation.

An understanding of the fluid response to these and other similar changes in acceleration can perhaps best be approached by considering the total problem as four chronological segments. The first segment of the problem concerns the initial configuration of the liquid. The second segment is the dynamic behavior of the liquid/vapor interface immediately following application of a new acceleration. The third segment is concerned with the nature of the resulting liquid flow from one end of the tank to the other. The fourth segment, about which little can be said at present, includes the turbulent splashing of the liquid once it reaches the end of the tank and the subsequent approach to quiescence.

1. Surface Shape

Techniques necessary for describing the surface of a quiescent liquid are available. The Young-Laplace equation:

$$p_2 - p_1 = \sigma\left(\frac{1}{R_1} + \frac{1}{R_2}\right), \qquad [1]$$

which relates the pressure difference across a liquid free surface, at any point, to the surface tension, σ, and the radii of curvature at that point, R_1 and R_2, was deduced from physical arguments by Young in 1804 and derived mathematically by Laplace shortly thereafter. If the hydrostatic pressures are expressed as functions of position, a nonlinear partial differential equation describing any static interface between two fluids under the joint influence of gravity (or an acceleration field) and surface tension is obtained.

Although no general solution to the resulting equation has ever been found, Adams developed a numerical method of solution for the case of axial symmetry around 1855, and Bashforth applied his method to the calculation of surface shapes for a large number of cases during the years 1855 through 1857 (Ref 1). Extensions of the Bashforth and Adams work have been made by Fordham (Ref 2), who interpolated more detail into the tables, Staicopolus (Ref 3) and Satterlee and Chin (Ref 4), who used digital computers to solve the axisymmetric equation, and Jurney (Ref 5), who adapted the Bashforth and Adams tables to obtain axisymmetric interface shapes for known amounts of liquid contained in axisymmetric vessels of various shapes.

A significant recent contribution has been made by Larkin (Ref 6 and 7), who extended Adams' method to the more general case of nonsymmetric interfaces and accelerations arbitrary in both direction and magnitude, and used the digital computer to calculate surface shapes for a number of cases. Larkin has also found good agreement between his data and experimental results that have not yet been published.

In Section B, a linear approximation to the initial interface shape will be used because of the difficulty of incorporating more exact expressions into the otherwise linearized analysis.

2. Surface Dynamics

When the acceleration changes to a new value, the surface, since it no longer is in equilibrium, begins to move. The problem can be treated as one of constant vehicle acceleration with a static, nonequilibrium initial condition. As the surface relaxes from this initial condition, it assumes a complex wave shape, just as a membrane assumes a complex wave shape after it is distended and then released. (The surface is, in fact, much like a membrane, in that it is characterized by a surface tension that resembles the tension in a membrane stretched uniformly in all directions.) The surface waves might be either stable or unstable. If they are all stable, the surface will oscillate about a new position of equilibrium, whereas if any wave is unstable, the liquid will flow until it has changed places with the gas.

A good understanding of waves on flat liquid surfaces was obtained in the middle of the nineteenth century, primarily as a result of the efforts of Airy, Stokes, and Thomson (Ref 8, 9, and 10). The stability of flat surfaces with fixed boundaries was investigated by Maxwell (Ref 11) in 1878. Only in the last few years, however, has the dynamics of curved liquid surfaces been studied.

A variational approach presented by Concus (Ref 12) allowed the limits of stability of a curved, two-dimensional capillary surface to be found. This approach was extended by Satterlee and Reynolds (Ref 13) in 1964 to the study of the stability and dynamics of curved axisymmetric surfaces. The variational approach allowed the equations to be linearized about a curved, axisymmetric equilibrium surface, rather than about the plane equilibrium surface that had concerned earlier investigators.

A few recent investigations have applied these dynamic considerations to the problem of the response of liquid surfaces to changing accelerations. Moore and Perko (Ref 14) and Concus, Crane, and Perko (Ref 15) used variational methods to investigate the sudden application of an acceleration to an initially free-floating container. The approach consisted of initially neglecting surface tension and later attempting to enter it as a small perturbation, or smoothing term. Fung (Ref 16) considered the inverse problem of a suddenly removed acceleration or gravitational field. He followed the classical approach of solving equations linearized about a plane, and consequently was more successful in including surface tension in his analysis.

The classical approach will also be followed in Section B to look at the more general problem of surface response to any change in the magnitude or direction of the acceleration applied to a cylindrical, partially filled container of liquid.

It should be noted that viscous effects on liquid surface oscillations have been considered by Harrison (Ref 17), Bellman and Pennington (Ref 18), Chandrasekhar (Ref 19 and 20), Reid (Ref 21), and Willson (Ref 22). Consideration of viscous effects complicates a linearized analysis considerably, of course, since the viscous terms are themselves nonlinear.

3. Liquid Flow

If the initial surface is unstable when subjected to the new acceleration, its perturbations will grow and result in flow of the two fluids through and around each other until they come to equilibrium at new locations in the tank. Several experimental programs have been concerned with the detailed nature of these flows.

The first experimental investigations of the development of surface instabilities and subsequent fluid flow were made by simply accelerating liquid containers downward for short distances (Ref 23 and 24). Since the advent of drop towers, however, experiments have been performed in these facilities because of the longer test durations possible and the more nearly constant accelerations that can be obtained.

Two basically different types of liquid settling experiments have been performed in drop towers. In one program (Ref 25), the test vessels always fell dreely during the first second or so of drop, allowing nearly spherical liquid surfaces to form, and then were accelerated downward, relative to free fall, for the final second of the test. In other programs (Ref 6, 26, 27, 28 and 29), the experimental packages were accelerated downward for the entire drop duration, and thus the settling flows were initiated from nearly flat liquid surfaces. Actually, neither limiting case -- flat or spherical surfaces -- is a valid representation of the nonuniformly curved capillary surfaces that would exist in typical propellant tanks during low earth orbital missions. Although such surfaces can be calculated, it has not been feasible to obtain them in the drop tower preliminary to downward acceleration. Therefore the analysis is a valuable means of extending the understanding gained experimentally to more realistic situations that cannot be reproduced in a drop tower.

Section C describes the experimental programs reported in Ref 6, 26, 28, and 29 as well as some recent extensions of that work. The original program covered the range of settling Bond numbers from 0 to 400; a later phase of the program investigated the range of settling Bond numbers from 400 to 2000 and, in addition, specifically examined the effects of offaxis accelerations.

B. ANALYSIS

Consider two motionless, superposed fluids contained in a closed right circular cylinder (Fig. I-1).

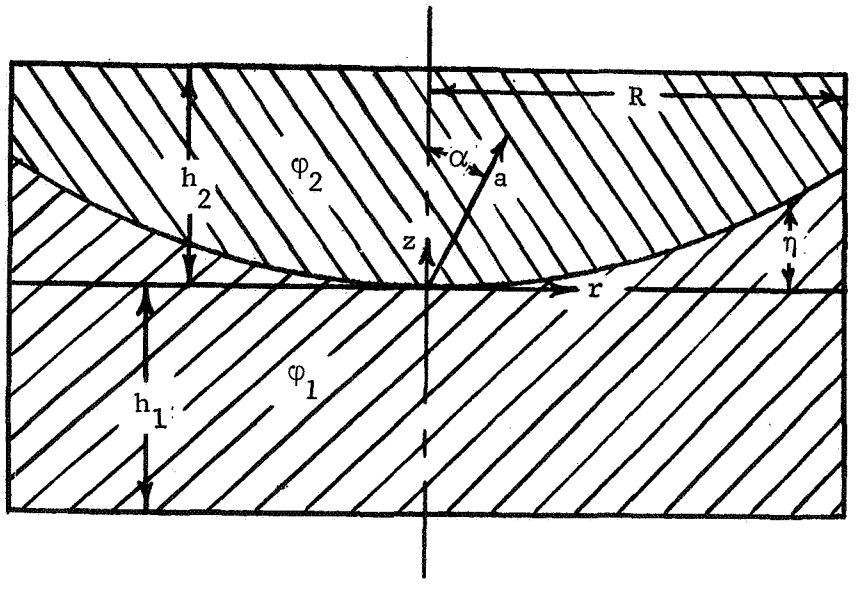


Fig. I-1 System of Interest

Initially the cylinder is accelerating at a rate a_o in a direction inclined at angle α_o to its axis. At time (t) = 0, the acceleration changes stepwise to a new magnitude, a, and direction, α. For simplicity, the two accelerations are taken at the same azimuthal angle. That is, $\vec{a}_o$, $\vec{a}$, and the cylinder axis all lie in

the same plane. Potential flow is assumed, and the equations will be linearized about the plane $z = 0$. As a result of the linearization, the analysis will be strictly valid only while the surface is approximately flat and horizontal and, consequently, only for cases where $\gamma \approx 90$ deg and α_o, $\alpha \approx 0$. The contact angle is further assumed to be constant.

1. Dynamic Equations

The velocity potentials $\varphi_1(r, \theta, z, t)$ and $\varphi_2(r, \theta, z, t)$ must each satisfy the continuity equation:

$$\nabla^2\varphi = 0, \qquad [2]$$

subject to the boundary conditions:

$$\left.\frac{\partial\varphi_1}{\partial r}\right|_{r=R} = \left.\frac{\partial\varphi_1}{\partial z}\right|_{z=-h_1} = \left.\frac{\partial\varphi_2}{\partial r}\right|_{r=R} = \left.\frac{\partial\varphi_2}{\partial z}\right|_{z=h_2} = 0, \qquad [3]$$

and the general surface condition:

$$\left[\frac{D}{Dt}(z - \eta)\right]_{z=\eta} = 0. \qquad [4]$$

Expanding D/Dt in terms of the space derivatives of φ_1, and then of φ_2, and linearizing about $z = 0$, gives:

$$\frac{\partial\eta}{\partial t} = \left.\frac{\partial\varphi_1}{\partial z}\right|_{z=0} = \left.\frac{\partial\varphi_2}{\partial z}\right|_{z=0}. \qquad [5]$$

Velocities were taken to be small quantities in the linearizations because of the quiescent initial conditions and the restriction on η. Equations [4] and [5] are often referred to as kinematic conditions since they relate the surface motion to the velocity of the fluid at the surface.

The most general solutions of Eq [2] consistent with Eq [3] and [5] are:

$$\varphi_i = F_i(t) \pm \sum_{n=0}^{\infty} \sum_{m=1}^{\infty} A_{m,n} \frac{\cosh k_{m,n}(z \pm h_i)}{\sinh k_{m,n} h_i} J_n(k_{m,n} r)$$

$$\left[B_n \sin n\theta + C_n \cos n\theta\right] f'_{m,n}(t), \qquad [6]$$

where

Plus signs are taken with i = 1;

Minus signs with i = 2;

$f'_{m,n}(t)$ are functions of time to be determined.

The additive functions of time $F_i(t)$ could have been omitted since they have no physical significance. They will not be seen again until the final equations, where the reason for emphasizing the possibility of their existence will be clear.

Eigenvalues, $k_{m,n}$, are defined by:

$$J'_n(k_{m,n}R) = \frac{n}{k_{m,n}R} J_n(k_{m,n}R) - J_{n+1}(k_{m,n}R) = 0. \qquad [7]$$

Using Eq [5], η can now be expressed as:

$$\eta = \sum_{n=0}^{\infty} \sum_{m=1}^{\infty} A_{m,n} k_{m,n} J_n(k_{m,n}r) \left[B_n \sin n\theta + C_n \cos n\theta\right] f_{m,n}(t) + \xi(r,\theta), \qquad [8]$$

where ξ is to be determined.

The pressure difference across the surface is given by the Young-Laplace equation, Eq [1]:

$$p_2 - p_1 = \frac{\sigma}{r}\left\{\frac{\partial}{\partial r}\left[r\zeta(r,\theta)\,\frac{\partial\eta}{\partial r}\right] + \frac{\partial}{r\partial\theta}\left[\zeta(r,\theta)\,\frac{\partial\eta}{\partial\theta}\right]\right\},$$

where

$$\zeta(r,\theta) \equiv \left[1 + \left(\frac{\partial\eta}{\partial r}\right)^2 + \left(\frac{\partial\eta}{r\partial\theta}\right)^2\right]^{-\frac{1}{2}}.$$

The linearizations imposed above result in approximating $\zeta(r,\theta)$ by unity, so that the pressure jump across the surface is linearized to:

$$p_2 - p_1 = \frac{\sigma}{r}\left[\frac{\partial}{\partial r}\left(r\,\frac{\partial\eta}{\partial r}\right) + \frac{1}{r}\,\frac{\partial^2\eta}{\partial\theta^2}\right]. \qquad [9]$$

If the pressures are expressed as functions of position and of the time derivatives of the velocity potentials, using Bernoulli's equation, Eq [9] becomes (after linearizing again):

$$-\frac{\sigma}{r}\left[\frac{\partial}{\partial r}\left(r\,\frac{\partial\eta}{\partial r}\right) + \frac{1}{r}\,\frac{\partial^2\eta}{\partial\theta^2}\right] + (\rho_1 - \rho_2)\,a\,(\eta\cos\alpha + r\sin\alpha\cos\theta)$$

$$+ \rho_1\left.\frac{\partial\varphi_1}{\partial t}\right|_{z=0} - \rho_2\left.\frac{\partial\varphi_2}{\partial t}\right|_{z=0} = \chi(t), \qquad [10]$$

where $\chi(t)$ is the arbitrary function of time from Bernoulli's equation.

The initial interface, $\eta_o \equiv \eta(r,\theta,0)$, can now be obtained by writing Eq [10] for the static equilibrium conditions that exist during the period $t < 0$:

$$\frac{\sigma}{r}\left[\frac{\partial}{\partial r}\left(r\,\frac{\partial\eta_o}{\partial r}\right) + \frac{1}{r}\,\frac{\partial^2\eta_o}{\partial\theta^2}\right] - \left[(\rho_1 - \rho_2)\,a_o\cos\alpha_o\right]\eta_o$$

$$= K + (\rho_1 - \rho_2)\,a_o\,r\cos\theta\sin\alpha_o, \qquad [11]$$

where $K \equiv \chi(0)$ is Bernoulli's constant.

This nonhomogeneous partial differential equation for η_o (r, θ) is a linearized form of the equation of capillarity. The exact equation has been solved numerically by Bashforth and Adams (Ref 1) for the axisymmetric case and by Larkin (Ref 6 and 7) for the three-dimensional case. The linearized analysis requires a linear expression for the initial interface, however.

The most general solution of Eq [11] is:

$$\eta_o = \sum_{j=0}^{\infty} \left[\delta_j \sin j\,\theta + \epsilon_j \cos j\,\theta\right] I_j(\beta_o r) - \frac{K}{\sigma\beta_o^2} - r \cos\theta \tan\alpha_o,$$

where

$$\beta_o^2 \equiv \frac{(\rho_1 - \rho_2)\, a_o \cos\alpha_o}{\sigma},$$

I = the modified Bessel function of the first kind.

The relationship between K and the Fourier coefficients δ_j and ϵ_j is determined by the choice of coordinates; if $\eta_o = 0$ at $r = 0$:

$$\frac{K}{\sigma\beta_o^2} = \epsilon_o.$$

The Fourier coefficients can be determined using the boundary condition:

$$\left.\frac{\partial\eta_o}{\partial r}\right|_{r=R} = \operatorname{ctn}\gamma,$$

giving finally the result:

$$\eta_o = \frac{\operatorname{ctn}\gamma\left[I_o(\beta_o r) - 1\right]}{\beta_o I_1(\beta_o R)} + \left[\frac{I_1(\beta_o r)}{\beta_o I_o(\beta_o R) - \frac{1}{R} I_1(\beta_o R)} - r\right]\cos\theta\tan\alpha_o. \quad [12]$$

Returning to the problem of the response of this initial surface to a new acceleration, it is seen that the time-dependent surface equation, Eq [10], allows solving for the functions $f_{m,n}(t)$. Taking $\partial/\partial t$ of Eq [10], substituting for $\partial\eta/\partial t$ from Eq [5], and requiring the series representations of φ_1 and φ_2 to satisfy the resulting homogeneous linear equation term by term gives:

$$f'''_{m,n}(t) + \omega_{m,n}^{2} f'_{m,n}(t) = 0, \qquad [13]$$

where

$$\omega_{m,n}^{2} \equiv \frac{k_{m,n}^{3}\sigma + (\rho_1 - \rho_2)\, a\, k_{m,n} \cos\alpha}{\rho_1 \operatorname{ctnh} k_{m,n}h_1 + \rho_2 \operatorname{ctnh} k_{m,n}h_2}. \qquad [14]$$

2. The Eigenvalue Problem and Stability Considerations

Equation [14], which was first derived (for the case of large h_1 and h_2) by Thomson (Ref 10) in 1871, allows the stability of liquid surfaces to be investigated, subject to the stated restrictions. Since the solutions of Eq [13] are:

$$f'_{m,n}(t) = \mu_{m,n} e^{i\omega_{m,n}t} + \nu_{m,n} e^{-i\omega_{m,n}t}, \qquad [15]$$

it is seen that any individual wave is stable (oscillatory) if its ω is real, and unstable (growing exponentially with time) if its ω is imaginary. Thus Eq [14] bears out the well-known fact that surfaces such as the one shown in Figure 1 are always stable if $\rho_1 > \rho_2$ and $a \cos\alpha \geq 0$. If, on the other hand, $\rho_1 > \rho_2$ and $a \cos\alpha < 0$ (or, equivalently, $\rho_1 < \rho_2$, $a \cos\alpha > 0$), perturbations with wave numbers $k_{m,n}$ less than $\left[(\rho_2 - \rho_1 \quad (a \cos\alpha)/\sigma\right]^{\frac{1}{2}}$ are unstable. Since the lowest eigenvalue $k_{m,n}$ is inversely proportional to the container radius R (see Eq [7]), there is a critical value of the container radius, for any acceleration and fluid properties, below which all the eigenvalues $k_{m,n}$ are greater than the critical wave number given by the stability criterion. The interface is consequently stable in these cases, even though the acceleration might be in an adverse direction.

This stability criterion can perhaps be more easily visualized if it is remembered that wavelength is equal to $2\pi/k$. Thus perturbations of an interface between two fluids subject to an adverse acceleration are unstable for sufficiently great wavelength, whereas waves whose lengths are less than the critical value $2\pi\left[(\rho_2 - \rho_1)(a \cos \alpha)/\sigma\right]^{-\frac{1}{2}}$ are stabilized by surface tension. In the case of a bounded surface, therefore, the surface is stable if its boundaries are sufficiently close together to prohibit the creation of any perturbations whose wavelengths would be greater than the critical value.

In following sections, it will be seen that it is generally most convenient to express quantities in terms of the dimensionless modified Bond number:

$$B_{\alpha R} \equiv \frac{(\rho_1 - \rho_2)\, a\, R^2}{\sigma} \cos \alpha.$$

With this Bond number, Eq [14] can be written as:

$$\frac{R\omega_{m,n}^2}{a \cos\alpha} = (k_{m,n}R)\left[1 + \frac{(k_{m,n}R)^2}{B_{\alpha R}}\right]\left(\frac{\rho_1 - \rho_2}{\rho_1 \operatorname{ctnh} k_{m,n}h_1 + \rho_2 \operatorname{ctnh} k_{m,n}h_2}\right) \quad [16]$$

where $B_{\alpha R}$ is negative for negative $a \cos \alpha$, and $k_{m,n} R$ can have only the discrete values given by Eq [7]. Instability is seen to exist for:

$$(k_{m,n}R)^2 < - B_{\alpha R};$$

or, alternatively,

$$\frac{1}{4\pi^2}\left(\frac{\mathscr{L}_{m,n}}{R}\right)^2 > - \frac{1}{B_{\alpha R}},$$

where $\mathscr{L}_{m,n}$ is the wavelength.

Directing our attention now to some specific wave-forms, stability criteria in the form of critical Bond numbers can be calculated. The fundamental mode has a wave number given by

$$k_{1,1} R = 1.84$$

and thus the fundamental mode is unstable for Bond numbers less than -3.39. Similarly, the wave numbers of the first five axisymmetric modes, and the corresponding critical Bond numbers, are:

1) $k_{1,0} = 3.83/R$, $(B_{\alpha R})_{CR} = -14.7$;

2) $k_{2,0} = 7.02/R$, $(B_{\alpha R})_{CR} = -49.4$;

3) $k_{3,0} = 10.17/R$, $(B_{\alpha R})_{CR} = -103.5$;

4) $k_{4,0} = 13.32/R$, $(B_{\alpha R})_{CR} = -178$;

5) $k_{5,0} = 16.47/R$, $(B_{\alpha R})_{CR} = -272.$

A few additional wave numbers and critical Bond numbers that will be of interest in later sections are:

1) $k_{2,1} = 5.33/R$, $(B_{\alpha R})_{CR} = -28.4$;

2) $k_{3,1} = 8.54/R$, $(B_{\alpha R})_{CR} = -72.9$;

3) $k_{4,1} = 11.71/R$, $(B_{\alpha R})_{CR} = -137$;

4) $k_{5,1} = 14.86/R$, $(B_{\alpha R})_{CR} = -221.$

It will be noticed that these considerations give, as the stability criterion for any cylindrically-bounded surface, a Bond number (based on radius) of -3.39, the critical Bond number for the fundamental mode. This value agrees with that found by Satterlee and Reynolds (Ref 13) for the case of 90-deg contact angle, the contact angle that the present analysis is linearized about. Satterlee and Reynolds found that the critical Bond number is a function of contact angle, symmetrical about 90 deg. For a contact angle of 0 or 180 deg, they found the critical Bond number to be -0.842, a value that was also found numerically by Bretherton (Ref 30) and Gluck and Gille (Ref 31), and experimentally by Hattori (Ref 32) and Masica et al. (Ref 33 and 34).

In addition to the question of the range of Bond numbers for which a given mode is unstable, an important question concerns the rate at which unstable modes grow, as a function of Bond number. Since unstable perturbations of the interface grow like $e^{\omega t} + e^{-\omega t}$ (see Eq [15], remembering that in unstable cases ω has imaginary values), the magnitude of ω is to some extent a measure of the ultimate growth rate, or degree of instability, of an unstable mode.

The limitation on this type of consideration is, of course, that unstable modes do not really grow exponentially with time for high values of time. The actual limit on the acceleration of any portion of the liquid surface is a cos α, the container acceleration. That is, the maximum growth of the liquid surface corresponds to liquid being left behind by the accelerating container. The apparent disagreement between this physical consideration and Eq [15] would seem to be due to the linearizations used to obtain Eq [15], which result in restricting its validity to small values of t, for which the surface displacement is small.

In spite of this limitation, it is of some value to investigate the degree of instability. As following sections will show, many aspects of the variations of surface response with Bond number can be better understood by considering the relative instabilities of the various axisymmetric modes. Figures I-2 thru I-5 are plots of $\frac{R\omega^2}{a \cos \alpha}$ against $B_{\alpha R}$, from Eq [16], for the first 10 axisymmetric modes. The approximation $\rho_2 \ll \rho_1$ (good for the case where fluid 1 is a liquid and fluid 2 is a vapor) has been made; thus they are plots of:

$$\frac{R\omega^2}{a \cos \alpha} = (k_{m,n}R) \left[1 + \frac{(k_{m,n}R)^2}{B_{\alpha R}}\right] \tanh \left[(k_{m,n}R)\left(\frac{h_1}{R}\right)\right],$$

for selected values of the ratio of liquid depth to tank radius. Since both ω^2 and a cos α are negative in the case of an unstable wave (given $\rho_1 > \rho_2$), the ordinate has positive values in each figure, while the Bond numbers of interest are negative.

It is seen in each of Fig. I-2 thru I-5 that for negative Bond numbers near zero none of the axisymmetric modes are unstable, as discussed above. At somewhat lower Bond numbers the first mode only is unstable. As Bond number continues to decrease, a region is reached where the first two modes are unstable, with the first more unstable than the second. At slightly lower Bond number, however, the curves for the first two modes cross, showing that at lower Bond numbers the second mode is more unstable than the first. Similarly, the third mode becomes unstable, then more unstable than the first mode, then more unstable than the second mode, and so on for higher modes, as Bond number continues to decrease.

This rather crude consideration of the relative instabilities, or growth rates, of various axisymmetric modes indicates that, at different settling Bond numbers, qualitatively different types of flow will result, depending on the number of unstable modes and their relative growth rates. Indeed, such variations in flow behavior were found, both analytically and experimentally, as discussed in later sections. The reasons for the transitions discussed there between different types of flow at different Bond numbers can to some extent be understood by considering Fig. I-2 thru I-5, along with Fig. I-6 and I-7, which show two different ways of plotting the Bessel function $J_o\left[\left(k_{m,0}R\right)\ (r/R)\right]$ for the first few eigenvalues $\left(k_{m,0}R\right)$. The Fourier-Bessel coefficients for each mode, which have not been included in these figures or in the analytical treatment thus far, will be evaluated in the following section.

Before proceeding to that section, note that while liquid depth (and, by extension, the shape of the container bottom) has no effect on the limit of stability of any mode, it does have a pronounced effect, in the case of very shallow liquids, on the degree of instability of the first few modes. The first few modes are less unstable in the case of very shallow liquids, and thus the intersections of their instability traces are moved to the left.

It should be remembered that the discussion of the last few paragraphs has been concerned only with the stability of axisymmetric perturbations of the interface, rather than with the entire question of interfacial stability. Not taken into account was the fact that the fundamental mode for the interface is not an axisymmetric mode. In the region $-3.39 > B_{\alpha R} > -14.7$, the fundamental mode is unstable even though all the axisymmetric modes are stable. The fundamental mode, however, is not readily excited by purely axial accelerations, so that it might be expected that it would only be observed after longer periods of time. This phenomenon will be discussed at greater length in later sections.

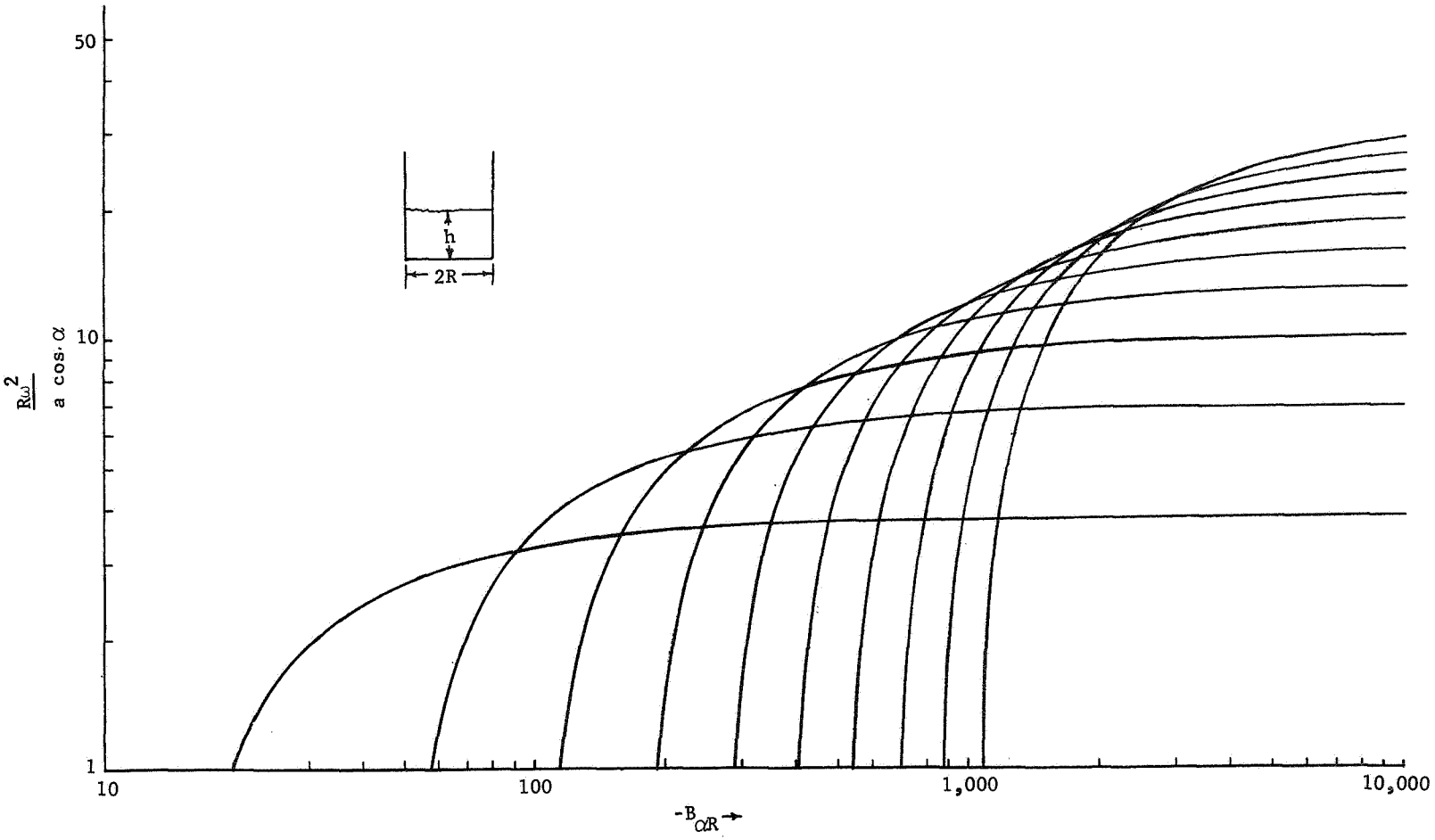


Fig. I-2 Degree of Instability of Axisymmetric Modes, $h/R \geq 1.0$

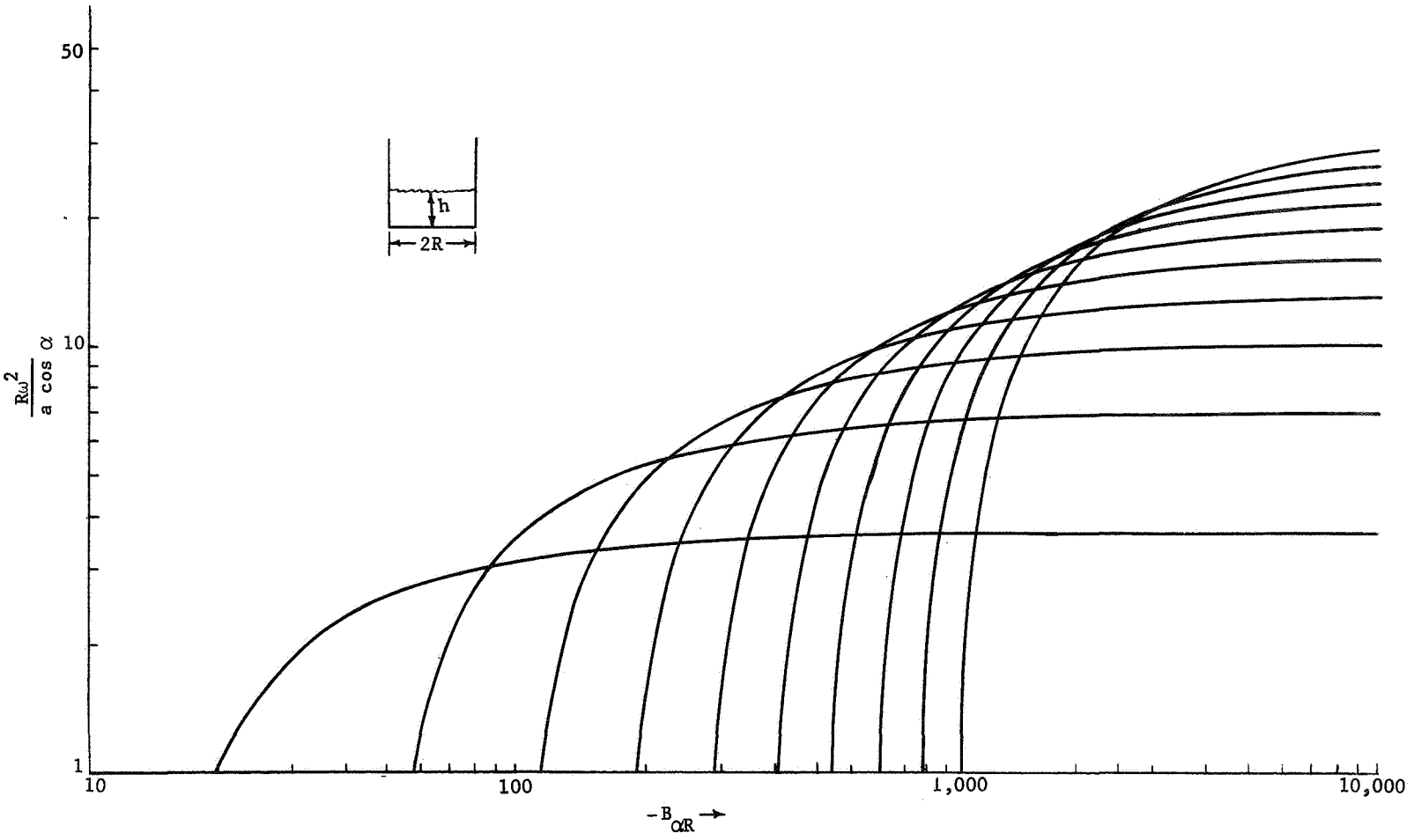


Fig. I-3 Degree of Instability of Axisymmetric Modes, h/R = 0.5

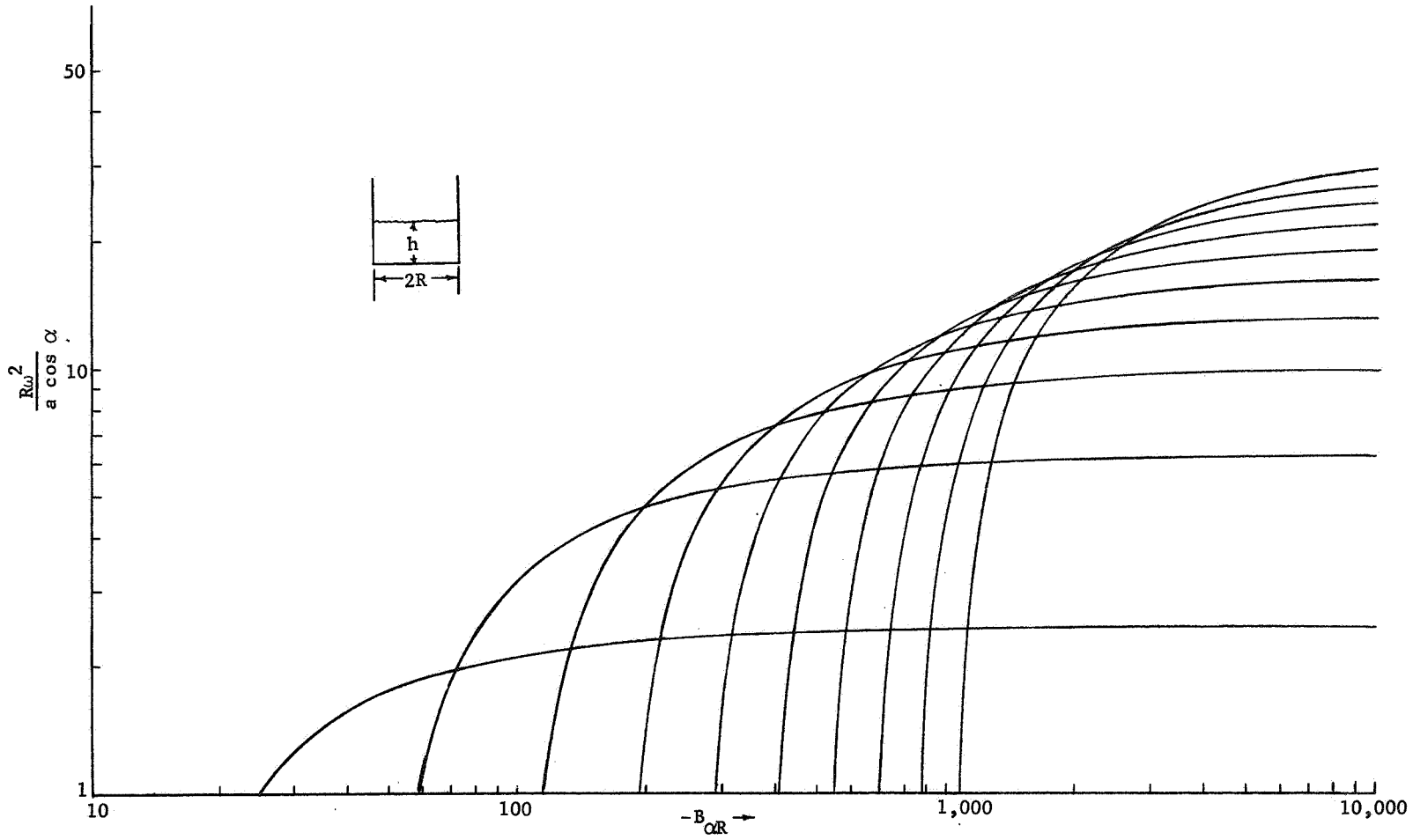


Fig. I-4 Degree of Instability of Axisymmetric Modes, h/R = 0.2

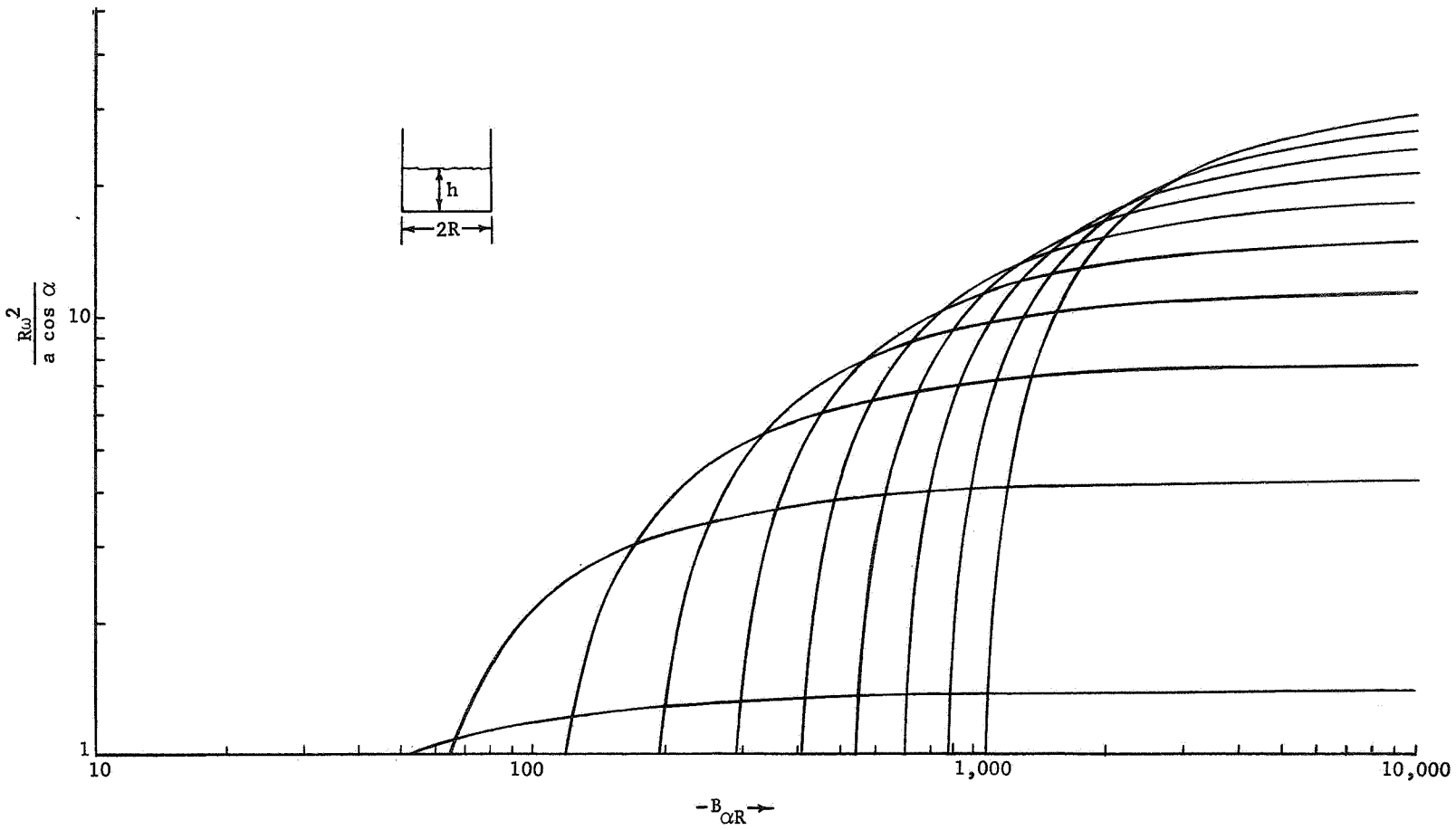


Fig. I-5 Degree of Instability of Axisymmetric Modes, h/R = 0.1

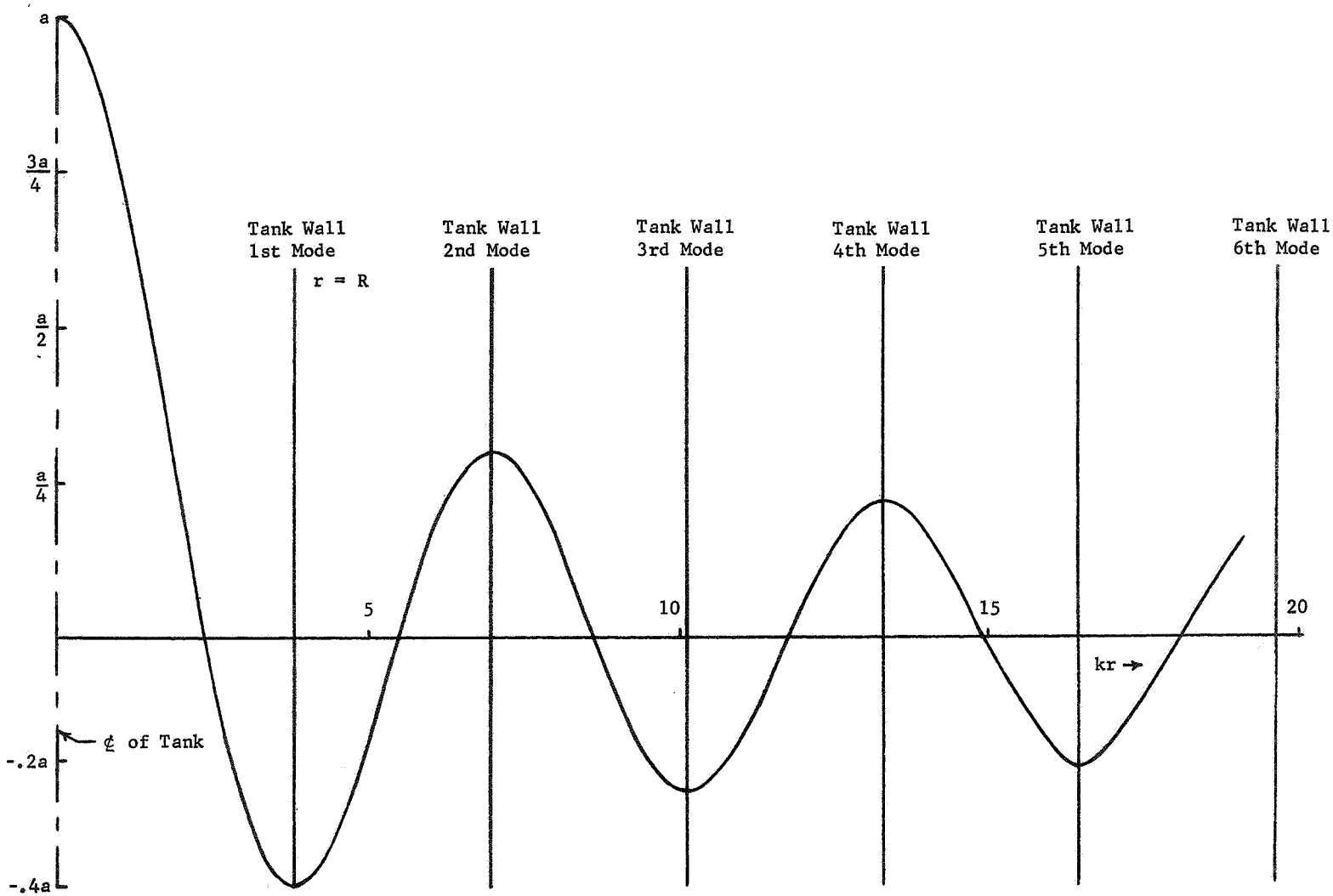


Fig. I-6 Axisymmetric Interface Shape

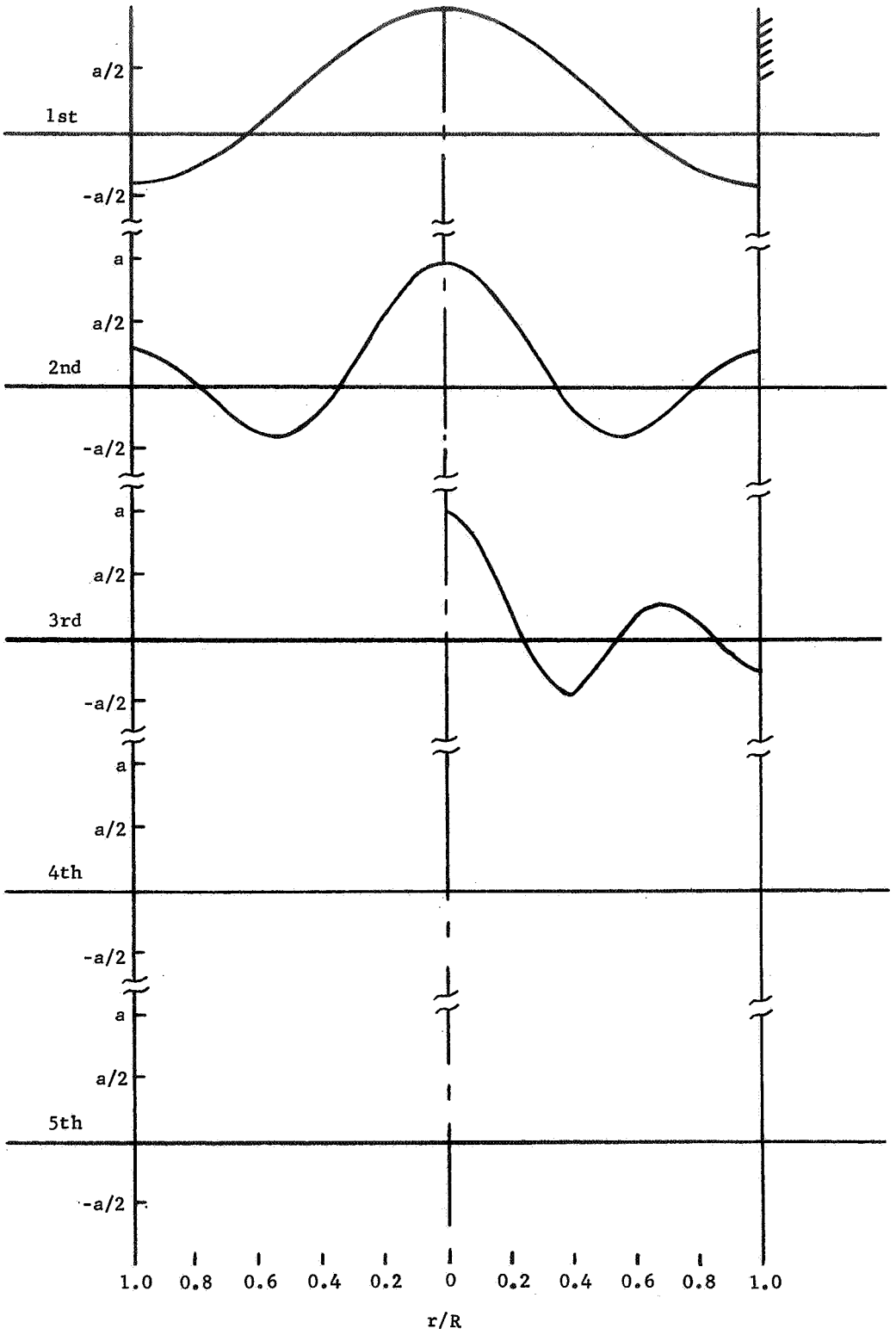


Fig. I-7 Axisymmetric Modes, Cross Section thru Axis

3. Response to an Applied Acceleration

Writing Eq [8] at t = 0 and substituting the resulting expression for ξ (r, θ) back into Eq [8], with $\mu_{m,n} = -\nu_{m,n}$ from the initial condition of zero velocity, allows η to be expressed as:

$$\eta(r, \theta, t) = \sum_{n=0}^{\infty} \sum_{m=1}^{\infty} \frac{d_{m,n} k_{m,n}}{i\omega_{m,n}} J_n(k_{m,n} r) \left[B_n \sin n\theta + C_n \cos n\theta\right]$$

$$\left(e^{i\omega_{m,n} t} + e^{-i\omega_{m,n} t} - 2\right) + \eta_o (r, \theta), \qquad [17]$$

where $d_{m,n} \equiv A_{m,n} \mu_{m,n}$. The Fourier-Bessel coefficients can be evaluated by writing Eq [10] for the changes that occur at t = 0. As the magnitude of the acceleration changes stepwise from a_o to a, and the direction from α_o to α, $\partial\varphi_1/\partial t$ and $\partial\varphi_2/\partial t$ must also change stepwise to nonzero values. The differences obey the equation:

$$(a_o \sin \alpha_o - a \sin \alpha)\, r \cos \theta + (a_o \cos \alpha_o - a \cos \alpha)\, \eta_o =$$

$$\left(\rho_1 \left.\frac{\partial \varphi_1}{\partial t}\right|_{z=t=0} - \rho_2 \left.\frac{\partial \varphi_2}{\partial t}\right|_{z=t=0}\right) \Big/ (\rho_1 - \rho_2).$$

Substituting for η_o, φ_1, and φ_2 gives the result:

$$(a_o \sin \alpha_o - a \sin \alpha)\, r \cos \theta$$

$$+ (a_o \cos \alpha_o - a \cos \alpha) \operatorname{ctn} \gamma \frac{\left[I_o(\beta_o r) - 1\right]}{\beta_o I_1(\beta_o R)}$$

$$+ (a_o \sin \alpha_o - a \cos \alpha \tan \alpha_o) \cos \theta \left[\frac{I_1(\beta_o r)}{\beta_o I_o(\beta_o R) - \frac{1}{R} I_1(\beta_o R)}\right] \qquad [18]$$

$$= \frac{\rho_1 F_1'(0) - \rho_2 F_2'(0)}{\rho_1 - \rho_2} + 2 \sum_{n=0}^{\infty} \sum_{m=1}^{\infty} i\omega_{m,n} d_{m,n}$$

$$\times \left(\frac{\rho_1 \operatorname{ctnh} k_{m,n} h_1 + \rho_2 \operatorname{ctnh} k_{m,n} h_2}{\rho_1 - \rho_2} \right) \left(B_n \sin n\theta + C_n \cos n\theta \right) J_n\left(k_{m,n} r\right).$$

Solving for the Fourier-Bessel coefficients by integrating over θ from 0 to 2π and over r from 0 to R (the orthogonality of the functions $J_n\left(k_{m,n} r\right)$ over this interval is due to Eq [7]), substituting the results into Eq [17], and nondimensionalizing gives the final result:

$$\frac{\eta}{R} = \left(B_{\alpha R} - B_{\alpha R_o} \right) \operatorname{ctn} \gamma \sum_{m=1}^{\infty} \frac{J_o\left(\lambda_{m,o} \frac{r}{R}\right) \tau_{m,o}(t)}{\left(B_{\alpha R} + \lambda_{m,o}^2 \right) \left(B_{\alpha R_o} + \lambda_{m,o}^2 \right) J_o\left(\lambda_{m,o}\right)}$$

$$+ \cos\theta \sum_{m=1}^{\infty} \frac{\left[\lambda_{m,1}^2 \left(B_{\alpha R} \tan\alpha - B_{\alpha R_o} \tan\alpha_o \right) + B_{\alpha R} B_{\alpha R_o} \left(\tan\alpha - \tan\alpha_o \right) \right] J_1\left(\lambda_{m,1} \frac{r}{R}\right) \tau_{m,1}(t)}{\left(B_{\alpha R} + \lambda_{m,1}^2 \right) \left(B_{\alpha R_o} + \lambda_{m,1}^2 \right) \left(\lambda_{m,1}^2 - 1 \right) J_1\left(\lambda_{m,1}\right)}$$

$$+ \operatorname{ctn} \gamma \frac{I_o\left[\left(B_{\alpha R_o} \right)^{\frac{1}{2}} \frac{r}{R} \right] - 1}{\left(B_{\alpha R_o} \right)^{\frac{1}{2}} I_1\left[\left(B_{\alpha R_o} \right)^{\frac{1}{2}} \right]}$$

$$+ \cos\theta \tan\alpha_o \left\{ \frac{I_1\left[\left(B_{\alpha R_o} \right)^{\frac{1}{2}} \frac{r}{R} \right]}{\left(B_{\alpha R_o} \right)^{\frac{1}{2}} I_o\left[\left(B_{\alpha R_o} \right)^{\frac{1}{2}} \right] - I_1\left[\left(B_{\alpha R_o} \right)^{\frac{1}{2}} \right]} - \frac{r}{R} \right\}, \qquad [19]$$

where

$$B_{\alpha R} \equiv \frac{(\rho_1 - \rho_2) a R^2}{\sigma} \cos\alpha,$$

$$B_{\alpha R_o} \equiv \frac{(\rho_1 - \rho_2) a_o R^2}{\sigma} \cos\alpha_o,$$

$\lambda_{m,n} \equiv$ the eigenvalues of $J_n'(\lambda_{m,n}) = 0$,

$$\omega_{m,n} \equiv \left\{ \frac{a}{R} \left[\lambda_{m,n} + \frac{\lambda_{m,n}^3}{B_{\alpha R}} \right] \left[\frac{(\rho_1 - \rho_2) \cos\alpha}{\rho_1 \operatorname{ctnh}\left(\lambda_{m,n} \frac{h_1}{R} \right) + \rho_2 \operatorname{ctnh}\left(\lambda_{m,n} \frac{h_2}{R} \right)} \right] \right\}^{\frac{1}{2}}$$

$$\tau_{m,n}(t) \equiv e^{i\omega_{m,n} t} + e^{-i\omega_{m,n} t} - 2.$$

In the case of off-axis accelerations, solution [19] is qualitatively different for different contact angles. The axisymmetric solution is proportional to ctn γ, and hence does not vary qualitatively with contact angle. The θ-dependent terms are independent of contact angle, however, and therefore the relative magnitudes of the two portions of the overall solution, and the nature of the superposition, cannot be investigated in general.

If the contact angle were taken to be much different from 90 deg, the axisymmetric portion of the solution would overwhelm the θ-dependent terms (for small α). Thus the investigation of the analytical results should be restricted to contact angles quite near 90 deg. The value of the analytical results obtained for these contact angles will somewhat depend on the extent to which they resemble experimental results obtained for other contact angles.

4. The Axisymmetric Case

Because of the impossibility of investigating Eq [19] in general, attention will first be concentrated on the axisymmetric portion of the solution, before proceeding to a consideration of the consequences and implications of the off-axis terms. In discussing the axisymmetric case, it should be remembered that the problem of interest is now restricted to purely axial accelerations, $\alpha \equiv \alpha_o \equiv 0$, and perfectly cylindrical containers.

The axisymmetric portion of the solution, Eq [19], was investigated for a large number of cases, using a digital computer to find the sum of the first 20 terms of the series. Good convergence was obtained by the 20th term for all the cases investigated. The computer program was written for a liquid/vapor system, $\rho_1 \gg \rho_2$, assuming a deep liquid, $h_1/R > 1$. In all of the cases investigated, the initial Bond number, B_{R_o}, was positive or zero, and the settling Bond number, B_R, was negative. The discussion of the results in this section will be predicated on the liquid wetting the wall ($\theta < 90$ deg), although the results are equally applicable to nonwetting liquids. It is interesting to notice that everything is turned upside down if the liquid doesn't wet the wall. For $\gamma > 90$ deg (ctn $\gamma < 0$), the dimensionless plots of Fig. I-8 thru I-16 are all inverted relative to plots of η against r. Instead of a layer of liquid climbing the walls, there would be a layer of gas descending along the walls. References to rising liquid domes would instead refer to descending domes of gas, and so forth.

The most complex and varied behavior was found for cases in which the initial Bond number was taken as 1000. This Bond number gave a nearly flat initial surface, representative of liquid surfaces in typical experimental vessels subject to normal earth gravity. Thus this series of results could be compared with the experiments reported in the experimental sections following, and in Ref 6 and 26.

Agreement was generally quite encouraging. A transition, with increasing magnitude of settling Bond number, from receding domes to growing spikes to growing domes with complex upper surfaces to hollow cylinders, which was found in the experimental program, was also indicated by the curves of Eq [19]. Some of the reasons for this variation of behavior were also brought out by the analytical results.

Two examples of curves that can be compared with the experimental results are shown in Fig. I-8 and I-9. In each of these figures, the development of surface waves from an initial curvature of the surface at the wall juncture can clearly be seen. The liquid right at the wall is initially elevated a small distance above the central region of the surface, in the case of a wetting liquid, by liquid/solid adhesion. As soon as the system is accelerated downward, this elevated liquid becomes an unstable wave, which grows in amplitude and propagates toward the centerline, pushing other waves in front of it. In Fig. I-8, the waves eventually form a dome, or spike, rising at the centerline of the tank, while at the lower Bond number of Fig. I-9, the resulting wave form is a hollow cylinder of liquid.

Additional cases were plotted, with the same initial surface, in which the settling Bond number magnitude was higher than any achieved during the original experimental program. The examples shown in Fig. I-10 and I-11 indicate that, at settling Bond numbers below -400, single hollow cylinders of liquid would continue to be observed. The diameter of the hollow cylinder relative to the wall diameter would increase with decreasing Bond number, and the wall thickness of the hollow liquid cylinder would decrease correspondingly. This behavior was verified in a later series of experiments, reported in Ref 28.

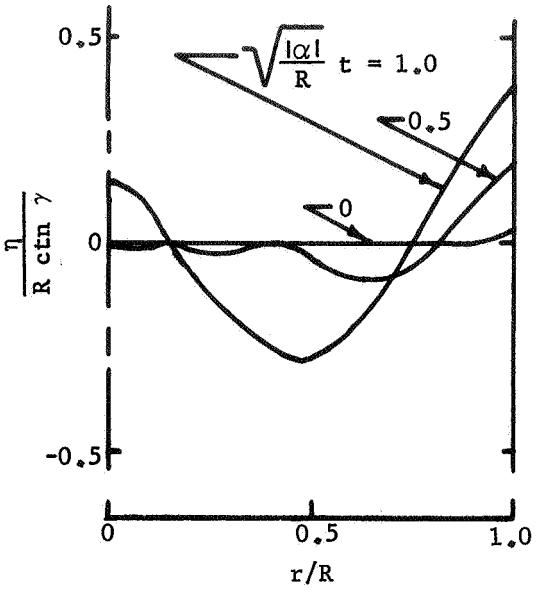


Fig. I-8 B_{R_o} = 1000, B_R = -30

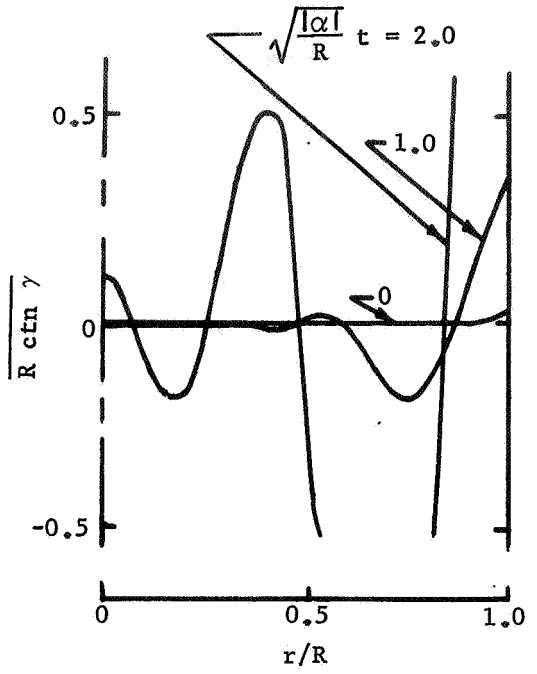


Fig. I-9 B_{R_o} = 1000, B_R = -200

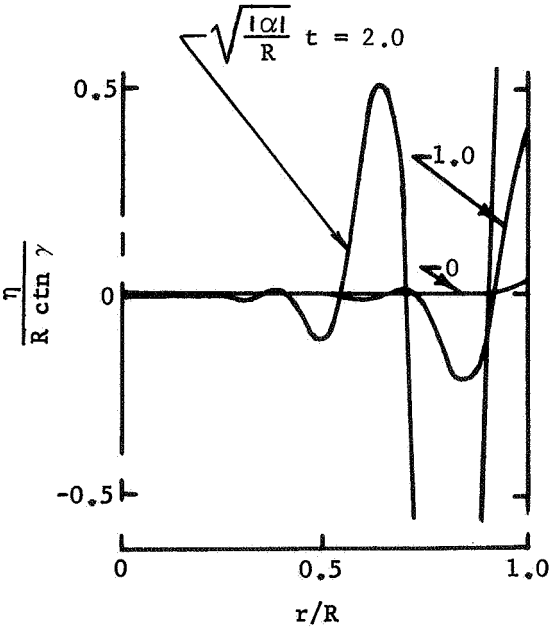


Fig. I-10 B_{R_o} = 1000, B_R = -600

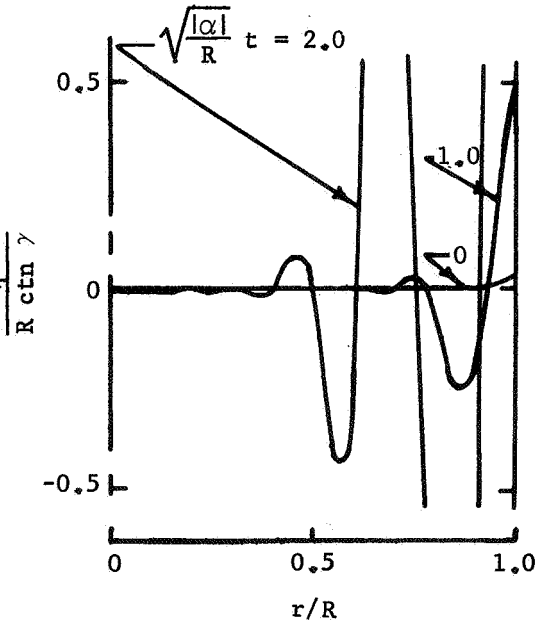


Fig. I-11 B_{R_o} = 1000, B_R = -1000

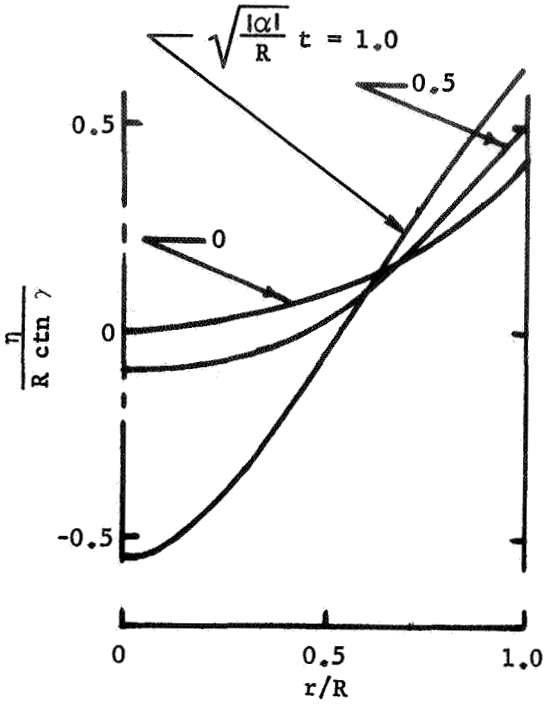


Fig. I-12 $B_{R_o} = 0$, $B_R = -10$

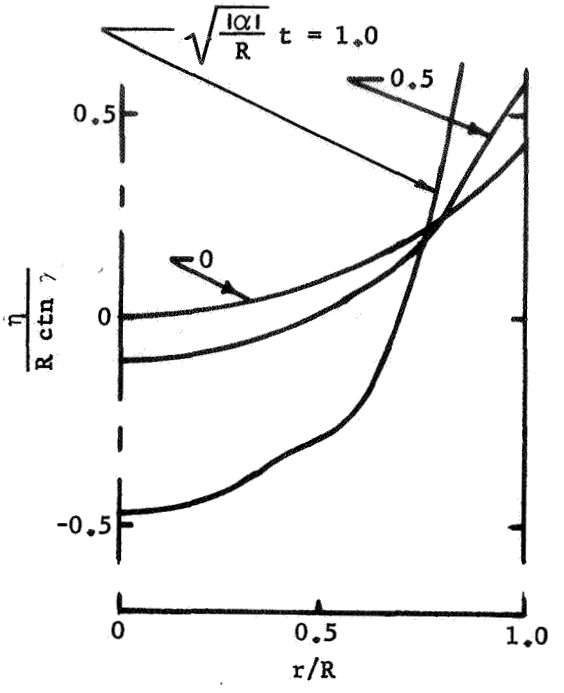


Fig. I-13 $B_{R_o} = 0$, $B_R = -100$

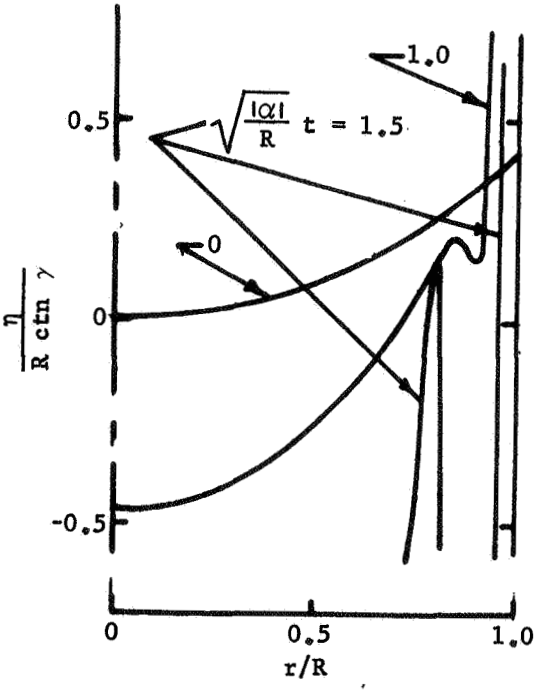


Fig. I-14 $B_{R_o} = 0$, $B_R = -2500$

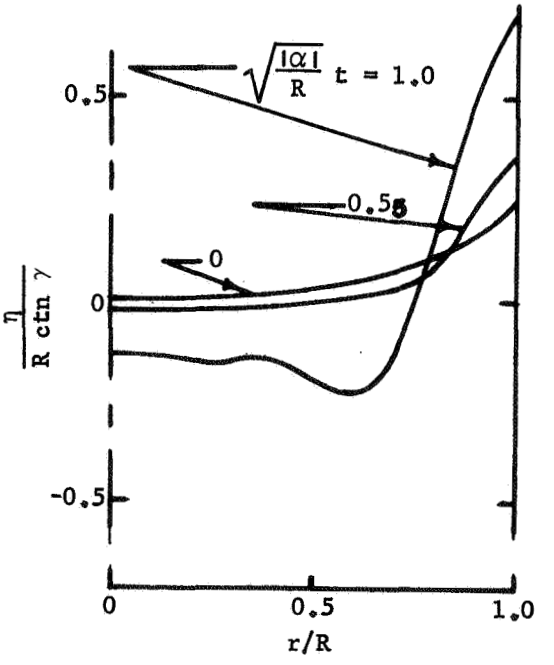


Fig. I-15 $B_{R_o} = 20$, $B_R = -100$

A series of plots were also made for the case of settling from a zero gravity (uniformly curved) initial interface, and compared with results of an experimental investigation of this case reported by Masica and Salzman (Ref 21). Some examples of this series of curves are shown in Fig. I-12 thru I-14. The curves in Fig. I-12 and I-13 correspond rather well to the reported experimental results. Although drop tower experiments at higher Bond number magnitudes were not reported, curves were plotted for settling Bond numbers to -2500. As shown in Fig. I-14, Eq [19] indicates that a circular wave could form at these Bond numbers and grow to form a hollow liquid cylinder just inside the liquid layer that climbs the wall. This indicated wave might be an anomaly resulting from the linearization; it would be interesting to know if such a wave can be observed experimentally.

A third series of plots was made for the case of settling from a low gravity nonuniformly curved initial surface. Experimental investigations of this case have not appeared in the literature to date, and would seem to involve appreciable difficulty. As shown in Fig. I-15 and I-16, Eq [19] indicates that, for an initial Bond number of 20, some of the features of the results for both spherical and flat initial surfaces are present. Although neither the complexity nor the variety observed in the results for an initial Bond number of 1000 are found in this case, there seems to be a distinct possibility that a dome of liquid could form in the center of the tank, with most of the flow occurring near the wall.

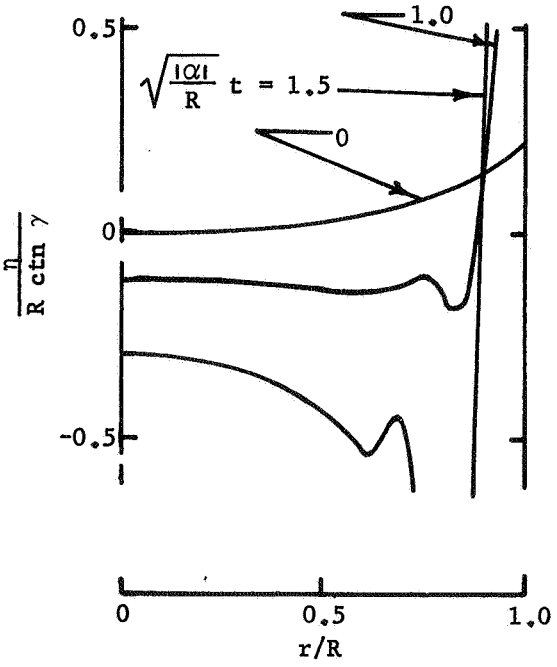


Fig. I-16 B_{R_o} = 20, B_R = -1000

5. The Effect of Offaxis Accelerations

A disturbing aspect of the axisymmetric solution investigated in the preceding section is the fact that the assumption of axial symmetry results in losing the lowest eigenvalues of the family of eigenfunctions $J_n'(k_{m,n}R)$. In the most general case, the velocity potentials, φ, in a cylindrical container must be described as linear superpositions of all the Bessel functions $J_n(k_{m,n}r)$ with the eigenvalues $k_{m,n}$ given by the boundary conditions $\partial\varphi/\partial r = 0$ at the cylinder wall, $r = R$. The lowest eigenvalue is the first zero of the eigenfunction $J_1'(k_{m,1}R) = 0$, or $k_{1,1}R = 1.84$. The corresponding limit of stability is $\rho a R^2/\sigma = -3.39$, as shown by Satterlee and Reynolds (Ref 13). If, however, it is assumed that accelerations are always purely axial, so the initial liquid configuration and its subsequent motion are axisymmetric, only Bessel functions of order zero are allowed in expressions for φ, and consequently the only remaining eigenvalues are those given by $J_o'(k_{m,o}R) = 0$. Thus the lowest eigenvalue is $k_{1,o}R = 3.83$, which results in a limit of stability that can be expressed as $\rho a R^2/\sigma = 14.67$, the value obtained by Maxwell (Ref 11) in 1878.

Some of the physical implications of these eigenvalue considerations can best be presented in the form of a simple gedankenexperiment. Consider a freely falling cylindrical container partially filled with liquid. The liquid is situated in one end of the container; its surface intersects the cylindrical wall of the container at an angle near 90 deg and is thus nearly flat. If the container is now slowly accelerated in a direction toward the liquid at a very gradually increasing rate, the liquid will eventually begin to flow to the opposite (lower) end of the tank. If the acceleration is purely axial, and if the solid/liquid/vapor system is otherwise perfectly axisymmetric, the surface can be expected to remain stable until an acceleration corresponding to a Bond number of -14.67 is reached, at which time and axisymmetric perturbation mode described by J_o (3.83 r/R) will begin to grow without bound. If, on the other hand, there is any departure from axial symmetry, such as a slight misalignment of the acceleration relative to the cylinder axis, the interface will remain stable only until a Bond number of -3.39 is reached, when the well-known fundamental mode will begin to grow without bound, resulting in flow up one side of the container.

With respect to the limits of stability of a liquid surface, therefore, the axisymmetric case is a singular one. Our interest is not directly centered on limits of stability, however, but rather on the more complex problem of surface response to slightly offaxis accelerations sufficiently large to cause axisymmetric instabilities. It is not immediately obvious, in the case of these higher accelerations, whether axisymmetric behavior is singular or a limiting case, or what the nature of the transition from purely axial to offaxis acceleration is. The degree to which the fundamental mode is manifest in the surface response, as a function of the initial interface configuration, settling Bond number, and acceleration angle, is also of interest.

In the experiments described in a later section, the fundamental mode was commonly observed in tests involving those vertical cylinders that could not be aligned with great precision, but it was not discerned when the containers were low L/D cylinders, with flat ends, which could be vertically aligned with much more precision. When the fundamental mode was observed, it generally began to grow much more slowly than the axisymmetric perturbations, but eventually resulted in the bulk of the liquid flowing up one side of the container, across the top, and back down the other side. Thus its influence on the long-term nature of the settling flow was considerable.

To investigate these problems in more detail, the complete solution given in Eq [19] was plotted, using the digital computer, for a number of cases. The computer summed the first 20 terms of the axisymmetric series and the first 10 terms of the θ-dependent series in Eq [19]. Good convergence was obtained in every case investigated.

In the examples of Fig. I-17 thru I-19, the contact angle was chosen rather arbitrarily to be 85 deg. The plots are intersections of the liquid surface with the plane θ = 0, 180 deg. A deep liquid/gas system $\left(h_1 / R > 1,\ \rho_1 \gg \rho_2\right)$ was assumed. The curves are all for the case $B_{\alpha R_o} = 250$, $B_{\alpha R} = -60$, at time $t = 2 (R/a)^{\frac{1}{2}}$.

In Fig. I-17, the cylinder is initially subject to an upward, axial acceleration. After t = 0, it accelerates downward and slightly to the left. As a result, the liquid tends to move up the right side of the cylinder.

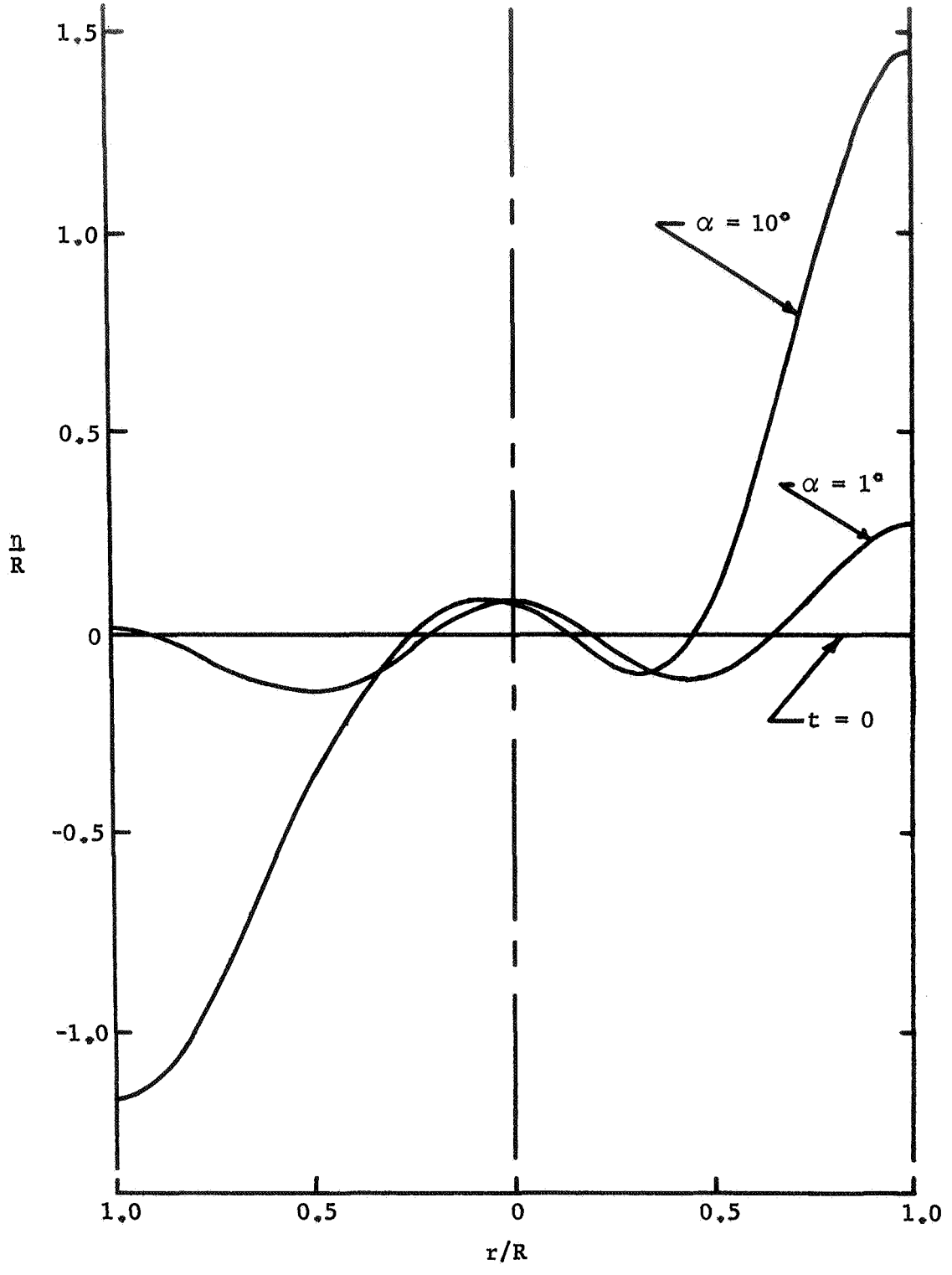


Fig. I-17 Analytical Results, α_o = 0 deg

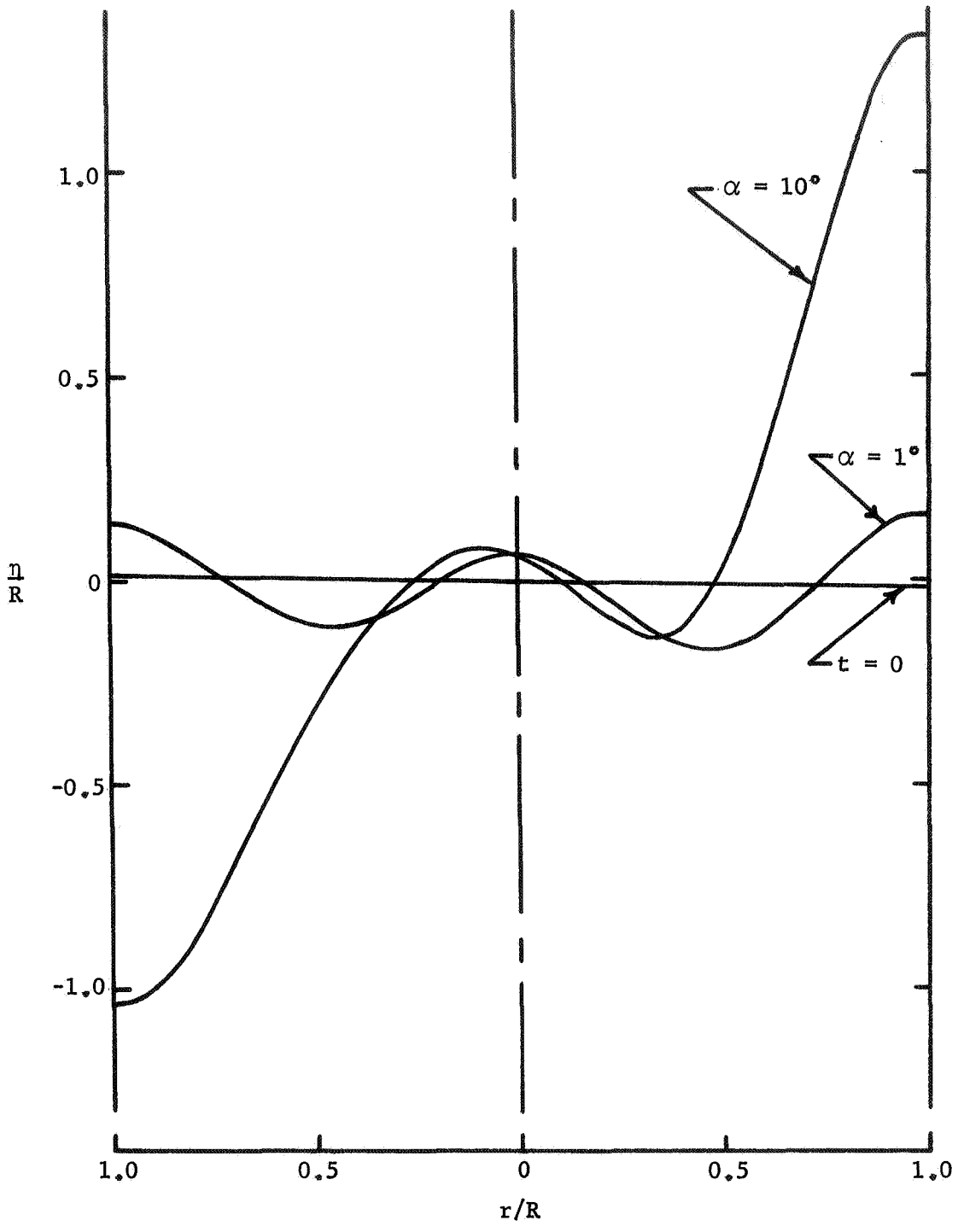


Fig. I-18 Analytical Results, α_o = 1 deg

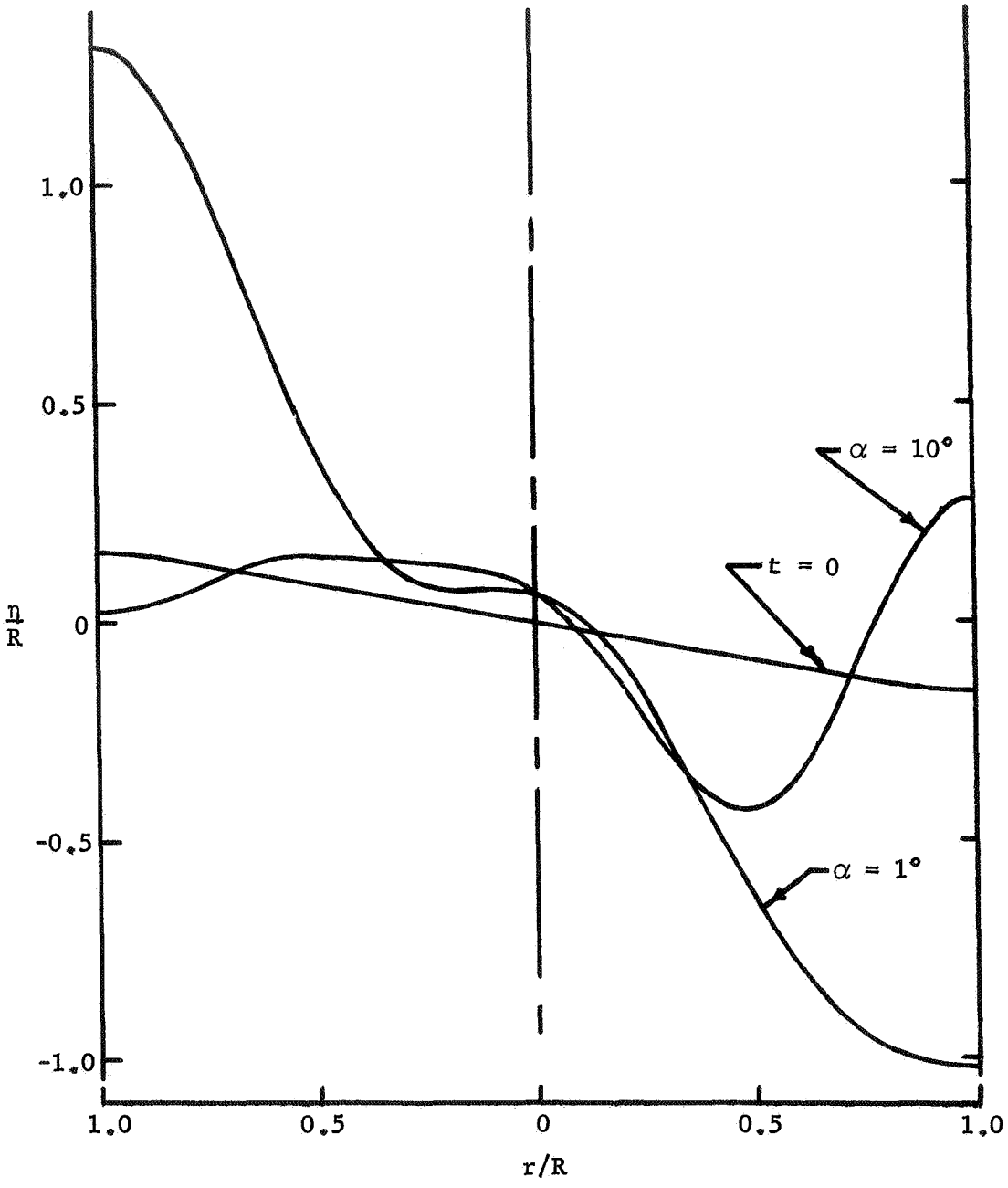


Fig. I-19 Analytical Results, α_o = 10 deg

In Fig. I-18 and I-19, the cylinder acceleration changes from upward and to the right to downward and to the left. The t = 0 surface gives a visual indication of the initial acceleration inclinations. In the case where the final leftward component is greater than the initial rightward component, the liquid moves up the right side of the cylinder, as in Fig. I-1. In the α_o = 10 deg, α = 1 deg case, however, the opposite happens. The initial elevation (as seen by the new acceleration) of the left side of the surface grows as the cylinder is accelerated downward, resulting in flow up the left side of the cylinder in spite of the fact that it is also accelerating to the left.

The two cases where the initial and final acceleration are antiparallel are more difficult to describe. The most pronounced response is found in the 10-deg case, where the bulk of the liquid seems to be moving to the left in spite of the fact that the liquid is climbing the wall on the right and descending on the left. The wall behavior, it should be pointed out, is entirely due to the contact angle assumption. Since $(\pi/2 - \gamma) < \alpha$, the initial solid/liquid/vapor intersection is above a plane, perpendicular to the acceleration direction and passing through the origin, on the right side and below it on the left. If $(\pi/2 - \gamma) > \alpha$, as in the 1-deg case shown (and most practical cases of interest), the initial intersection is everywhere above the same plane, and consequently the liquid climbs the wall everywhere.

It should be pointed out that if either α_o or α is nonzero, the analysis remains valid as $\gamma \to 90$ deg. In the axisymmetric portion of the solution, which was discussed in the preceding section, no surface response was indicated in the case of 90-deg contact angle, since in that case the equilibrium surface for any axial acceleration is a horizontal plane. Although the equilibrium might be unstable after an acceleration reversal, the axisymmetric analysis does not provide the small perturbations necessary before large waves can develop and flow occur. Because such perturbations would always result, eventually, from such extraneous sources as wall vibrations or convection currents, the linearized axisymmetric analysis can be said to be strictly valid only for contact angles near, but not too near, 90 deg. The latter part of the restriction does not apply in the case of offaxis accelerations, however, since the equilibrium surface shape is in general different for every value of β, the capillary constant. The only exception is a plane, which is the equilibrium surface shape for all values of β if γ = 90 deg and if the solid boundaries are everywhere parallel (at the solid/liquid/vapor intersection)

to the direction of acceleration. A plane is not an equilibrium surface shape for any other case (provided, of course, that the contact angle, γ, is uniform around the intersection). Therefore, the initial equilibrium surface cannot remain in equilibrium following an acceleration change, regardless of contact angle, if either α_o or α is nonzero.

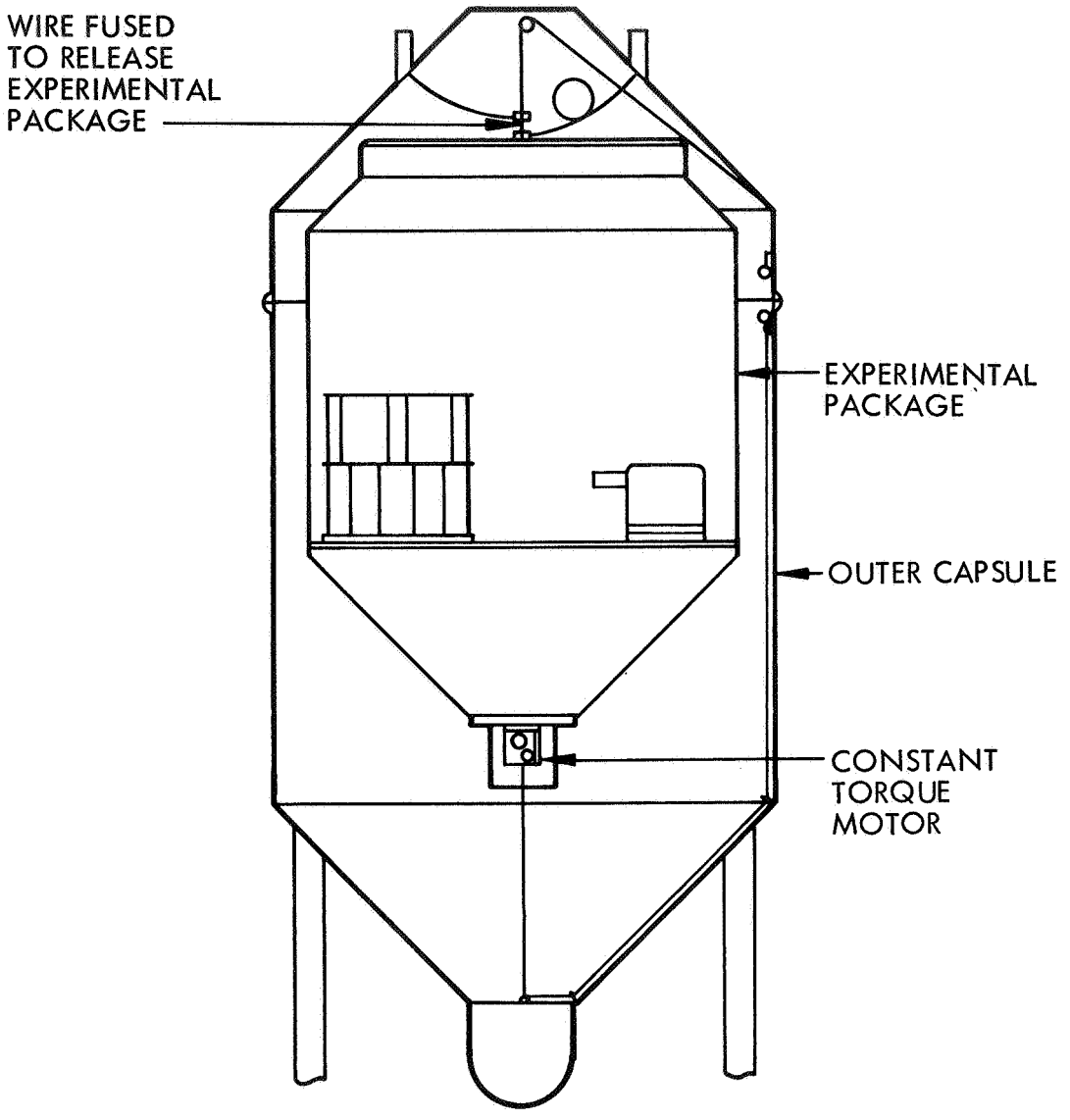
C. EXPERIMENTS

1. The Original Investigation: Settling Bond Numbers from 0 to 400

Experiments were performed in Martin-Denver's 75-ft drop tower, using constant force springs or cables from constant torque motors, extended between the experimental package and the outer capsule, to accelerate the experimental package downward relative to free fall.* The method is shown in Fig. I-20 and described in more detail by Paynter (Ref 35). Test vessels were transparent cylinders with inside diameters of 2.3, 4.7, 7.6, 9.5, 12.8, 13.2, 15.2, 16.7, and 29.2 cm, arranged in various combinations inside the experimental package. (See Ref 6 for pictorial information on some of the experimental equipment and methods.) The 12.8-, 15.2-, and 29.2-cm cylinders were plexiglass because of the breakage problem encountered with glass specimens of this size. The smaller cylinders were glass; the 13.2- and 16.7-cm cylinders were glass while they lasted. Initial accelerations ranged from 0.002 to 0.027 g. Test liquids were carbon tetrachloride, chloroform, Freon TF (trichlorotrifluoroethane), and methanol, with the bulk of the work being done with Freon TF because of its low specific surface tension (σ/ρ) with air, and its desirable handling properties. Bond numbers, based on specimen radius and initial acceleration, ranged from subcritical to 390. (The negative terminology, which was used in preceding sections to distinguish settling Bond numbers from initial Bond numbers, will be dropped in describing experimental work.)

Data were recorded using a Milliken camera operating at 200 frames per second. Films used were Kodak Plus-X and Ektachrome MS; the color film was used for most tests because it facilitated visual identification of many aspects of the complex flow patterns. Minute amounts of dye were used for the same reason; it was found that if just enough dye was used to give a barely discernible amount of color in the laboratory, the pictures would show a quite satisfactory liquid color.

*U.S. patent applied for by Martin Company.



(U.S. patent applied for by Martin Company)

Fig. I-20 Experimental Apparatus

Experiment technique ensured that the wire supporting the experimental package was fused immediately after release of the outer capsule. Otherwise, the liquid surface would have tended toward its usual free-fall shape before the fusing of the wire, and the type of flow being studied might not have developed. It was felt that meaningful settling experiments could be performed only if the liquid were quiescent at the time of application of the downward acceleration.

During this part of the program, 164 successful experiments were run at Bond numbers ranging from subcritical to 390. Since details of each of these experiments are tabulated in Ref 6, only the overall results will be reviewed in this report.

In this original program, there were strong indications that, because of limitations of the experimental apparatus, the actual acceleration of the experiment package decreased somewhat with time following capsule release. After this condition was corrected by constructing a larger outer capsule, as discussed in the following section, many of these experiments were repeated. No noticeable changes in the qualitative characteristics of the resulting flows were observed.

All of the settling tests performed in this original experimental program are represented in Fig. I-21, in which they are arranged according to Bond number at the start of each test. The horizontal position of the line corresponding to each Bond number indicates which of the five flow regimes described at the right side of the page applies to the observed phenomena. Each line shown in Fig. I-21 represents from one to six tests. The number of tests made at many of the listed Bond numbers is due in part to an attempt to find an influence, if any, of liquid filling level on the settling phenomena. No such influence was found. In several cases, the same Bond number (to two significant figures) was studied at two different acceleration levels, using test cylinders of different sizes or different test liquids. A more common occurrence was for the Bond number studied in one test to be within the range of Bond numbers studied in tests of a different series.

Figure I-22 presents more detailed descriptions of the rather wide range of fluid behavior that was grouped together as regime 5 in Fig. I-21. Analyses of only the best of the drop records have been included in Fig. I-22 because of the more detailed flow features that distinguished the various subregimes defined below the graph.

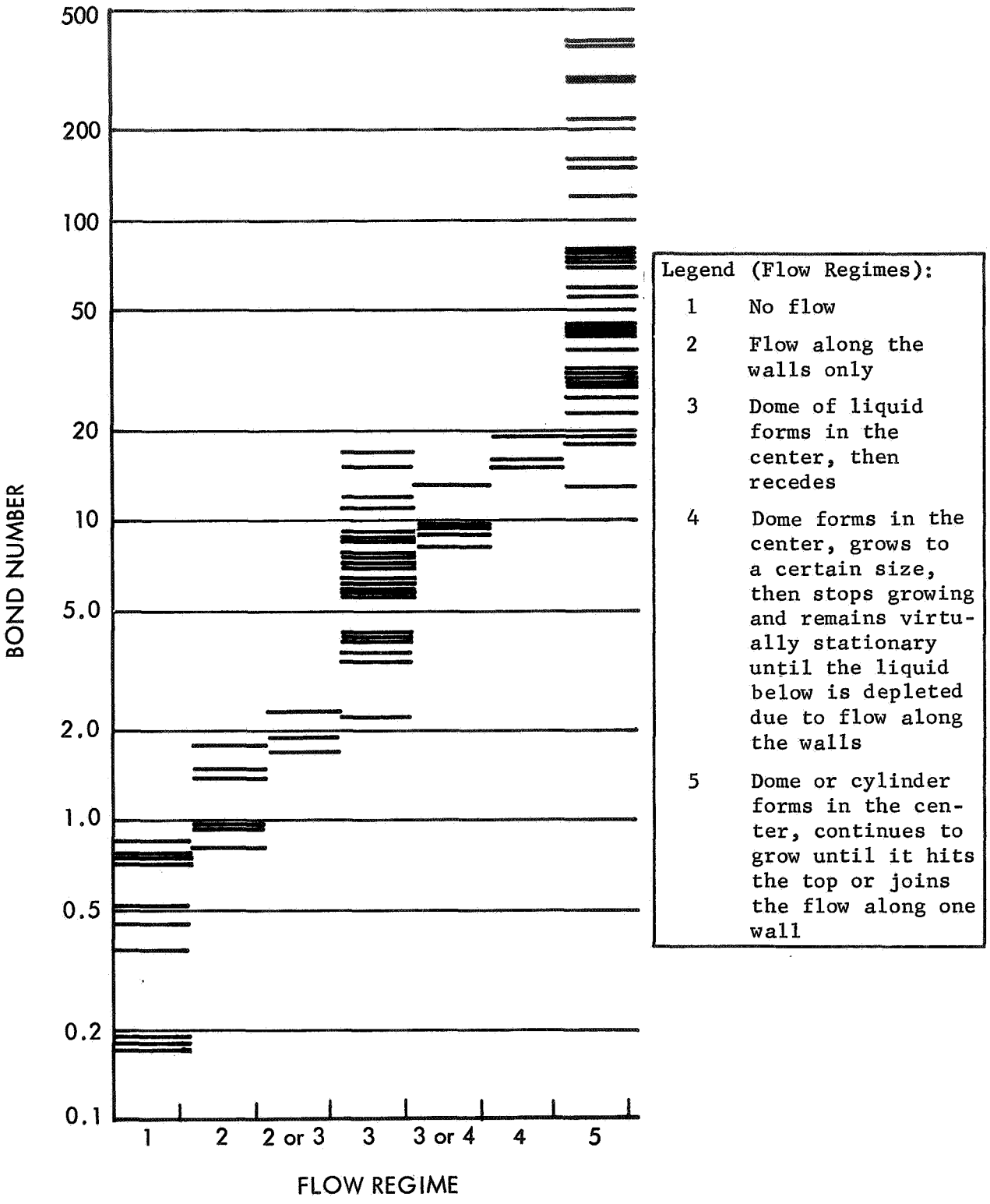
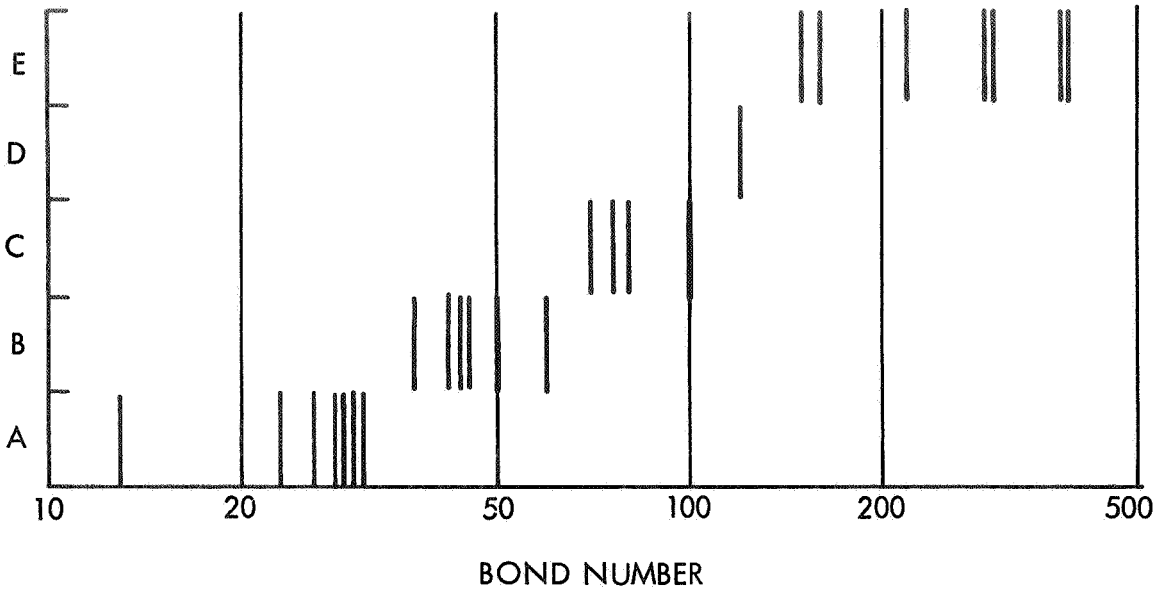


Fig. I-21 General Classification of the Observed Flows



Legend:

A	The liquid dome grows into a thin spike that eventually extends to the top of the tank. Effects of Helmholtz instability are seen if the spike L/D becomes large enough
B	A small depression forms in the center of the upper surface of the dome. Shortly after its formation, the depression turns inside out, becoming a small protuberance on the top surface of the dome. The protuberance grows rapidly in amplitude and diameter relative to the original dome until the two cannot be distinguished from each other. Together they form a column up the center of the cylinder, as in A
C	A depression forms in the center of the upper surface of the dome, similar to the depression observed in B but somewhat larger. The depression is present only temporarily, leaving behind a bubble or cavity inside the dome. No protuberance is seen to form following the breakup of the depression
D	In its formative stages, the cylinder has a complex upper surface characterized by concentric waves whose amplitudes become large with time. The eventual result is a broad dome with protuberance growing on its upper surface as in B
E	Same as D, except that the eventual result is a hollow cylinder

Fig. I-22 Additional Features of the Central Flow Observed in Certain Regime 5 Flows

Classifying a broad range of different flows as fitting one of a number of brief descriptions, as in Fig. I-21 and I-22, is obviously artificial. Nevertheless, such groupings as those shown seem to be the most concise and understandable presentation possible of the experimental program results. In addition, they allow some interesting comparisons to be made with the eigenvalue considerations of Paragraph 2 of Section B. The discussion and results of that paragraph provide reasons for the various types of phenomena, and the transitions between the different phenomena, shown in Fig. I-21 and I-22.

Primary weaknesses in these groupings of experimentally observed phenomena are at the boundaries between the different types of flow, as indicated in Fig. I-21. In general, there are always some uncertainties at the boundaries since they are, of course, not really boundaries at all. The actual physical phenomena undergo a continuous transition with Bond number. In a number of regions the liquid behavior can, to some extent, be described verbally; between these regions, there are other regions where the flow cannot be described so simply. These latter regions have been approximated as boundaries between the regions where the flow is capable of verbal description.

In addition to these unavoidable uncertainties, however, are a few others that deserve comment. There is some uncertainty at the boundary between regimes 2 and 3 because many of these tests were made with the smallest (2.3-cm) test cylinders at relatively high acceleration levels. The liquid domes were present in these small cylinders only for extremely brief intervals of time,* if at all; in addition, photographic resolution was not as good as in the large cylinders. The range of Bond numbers from 13 to 20 includes various types of behavior interspersed with each other, as can be seen in Fig. I-21. At Bond numbers 13, 15, and 19, different tests gave different types of behavior. Spikes were formed in some tests, while in others the dome did not grow past a certain maximum height. Once a dome attained a spike shape, the spike continued to grow.

---

*Time scale is given by the acceleration level and physical dimensions of the test vessel, as shown in the analysis presented in earlier sections; $t \sim (R/A)^{\frac{1}{2}}$ for similarity of results at any given Bond number, so higher accelerations and smaller physical dimensions in the experimental model both result in things happening faster.

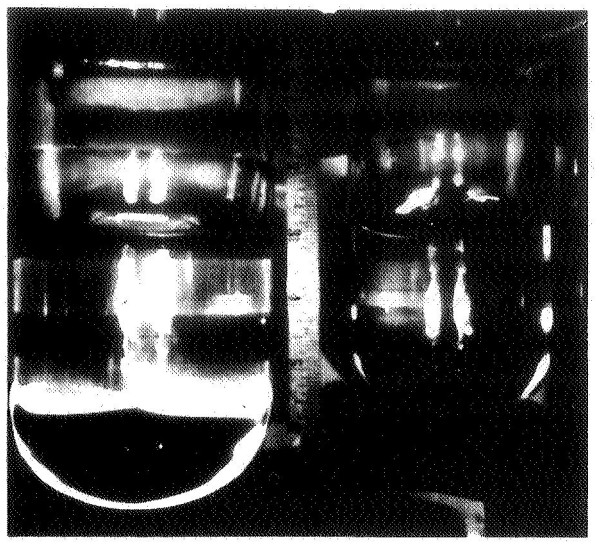
Figures I-23 thru I-25 show some specific examples of the various types of flow described as regions 3 thru 5 in Fig. I-21. Each illustration is a series of still photos reproduced from the motion picture record of a typical drop test. All three examples were chosen from a series of drops made with Freon TF and an initial acceleration of 0.016 to 0.017 g.

Figure I-23 shows a test specimen containing two cylinders with inside diameters of 7.6 and 9.5 cm. Bond numbers immediately following capsule release are consequently 20 and 31.

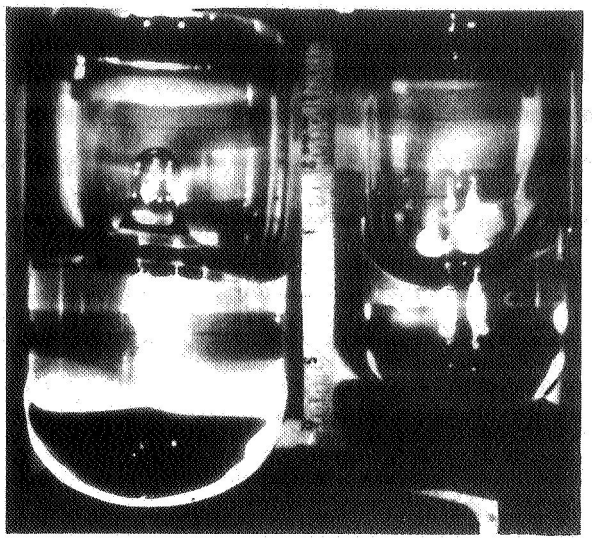
At 0.53 sec (Fig. I-23a), the liquid is climbing the walls of each tank. In addition, surface instability is manifested in the formation of domes rising in the central portion of each tank. In the smaller tank, the dome is already moving toward the right side of the tank.

At 1.06 sec (Fig. I-23b), the first thin layer of liquid flowing up the walls has reached the top of each tank and is beginning to flow radially inward along the top. The dome in the smaller tank has reached the wall on the right side, with the result that the major part of the flow is being established along that wall. Since the dome in the smaller tank has moved away from the central region of the interface, the interface is free to assume a curved shape, as it might in the case of a bubble or in a static zero-gravity situation. In the larger tank, the spike is growing almost vertically. In addition, surface tension is beginning to manifest itself in a pinching-off of the flowing column of liquid about 1-1/2 diameters below the top.

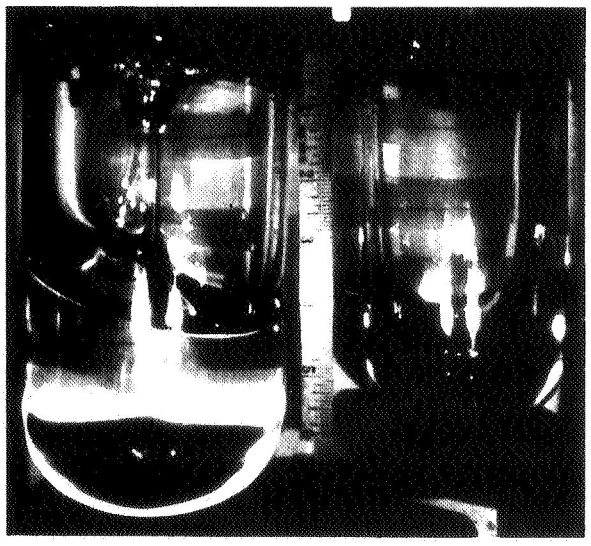
At 1.58 sec (Fig. I-23c), the major flow up the right side of the smaller tank has reached the top of the tank, proceeded across the top, and is beginning to splash back down. The column of liquid in the larger tank has almost reached the top and at the same time its base is beginning to move to the left, taking a large amount of liquid below with it. The surface tension has resulted in a sphere of liquid being almost separated from the remainder of the column. Ripples moving down the walls result from the initial thin layer that flowed up the walls, hit the top, rebounded, and is now setting up interference with the continuing flow up the walls.



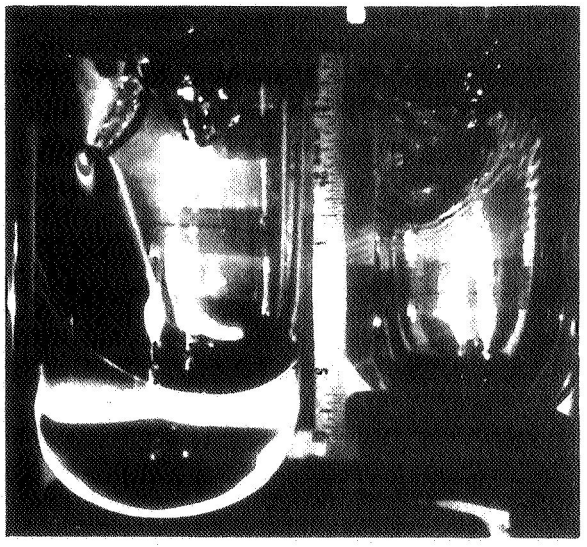
(a) 0.53 sec



(b) 1.06 sec

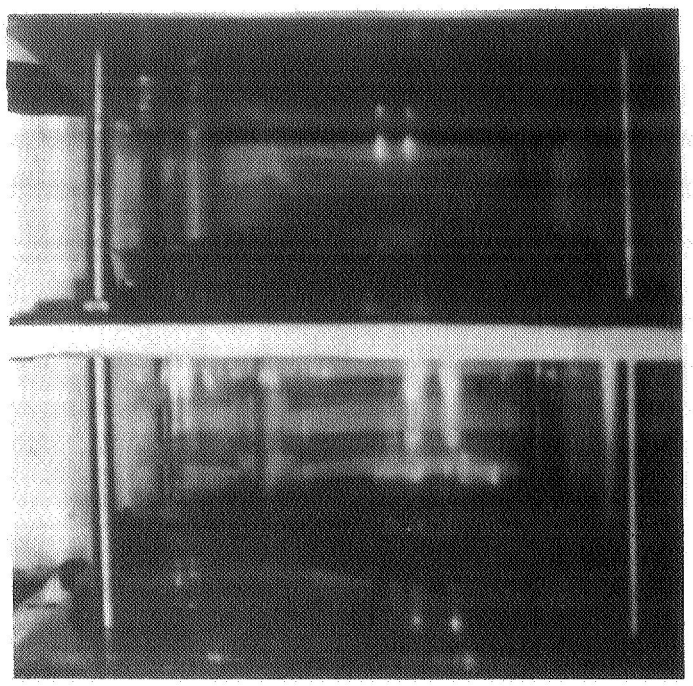


(c) 1.58 sec

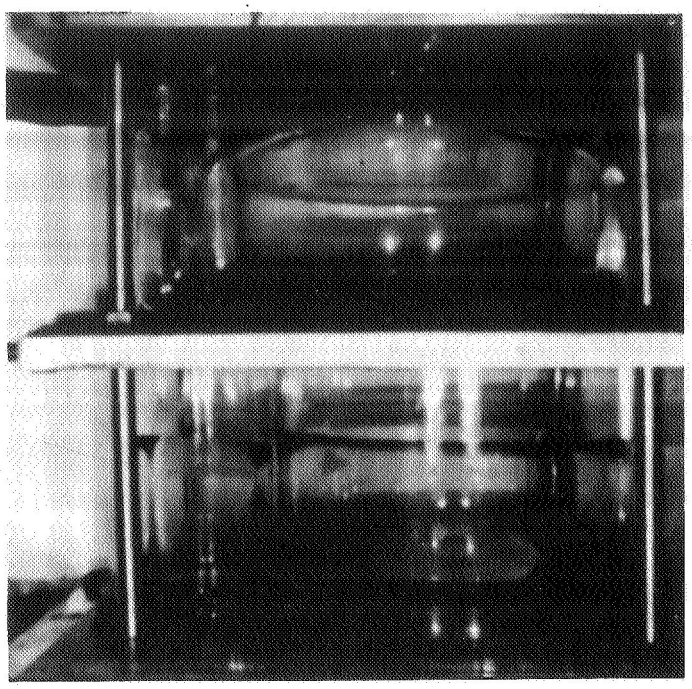


(d) 2.11 sec

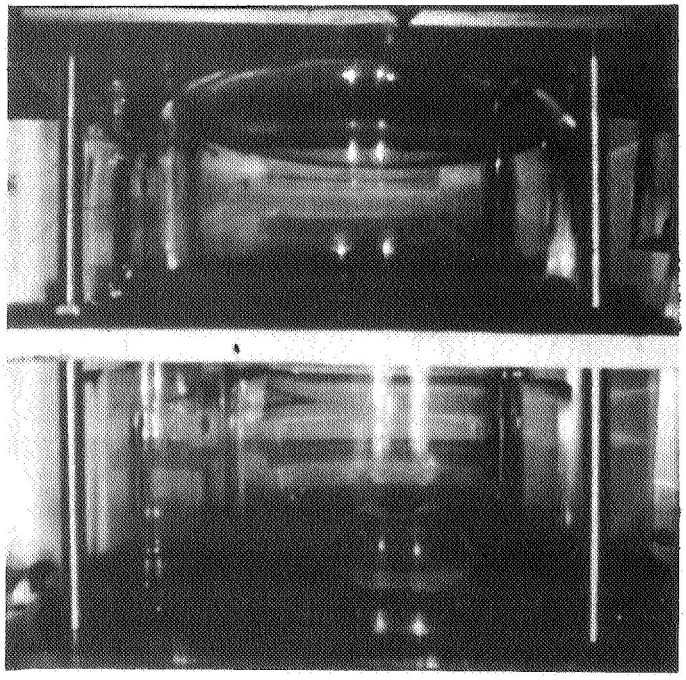
Fig. I-23 7.6- and 9.5-cm Cylinders at 0.016 g (Freon TF)



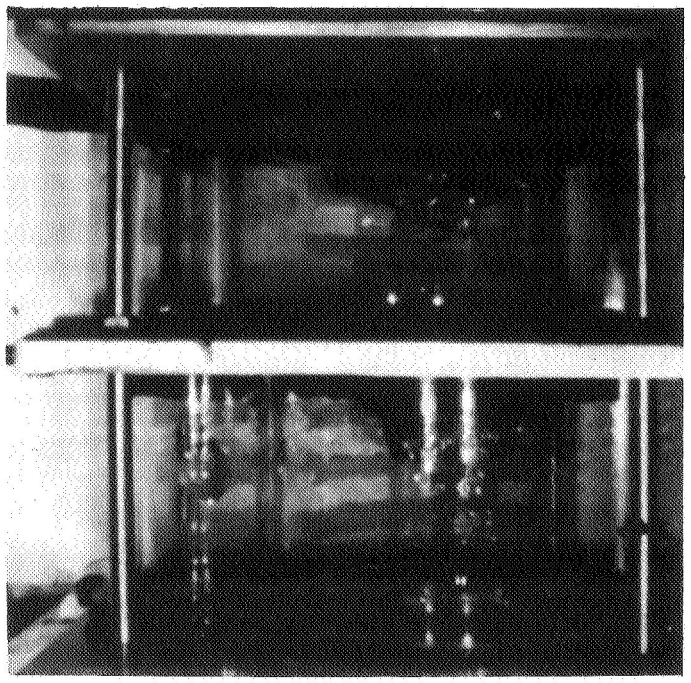
(a) 0.27 sec



(b) 0.77 sec

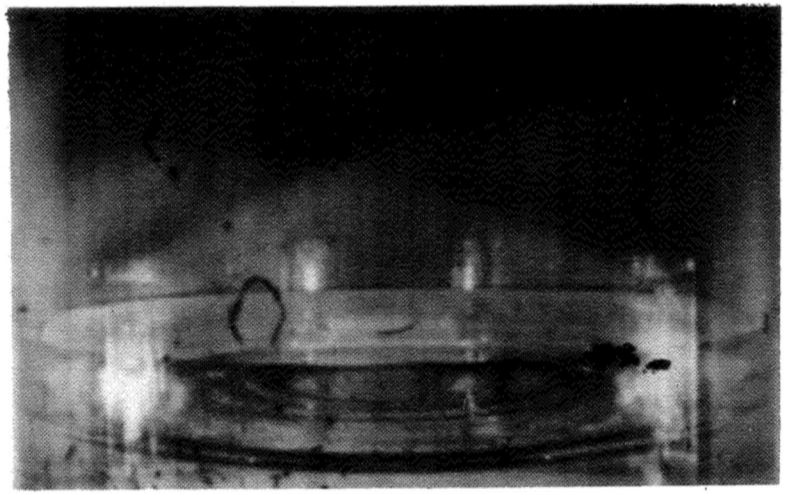


(c) 0.98 sec

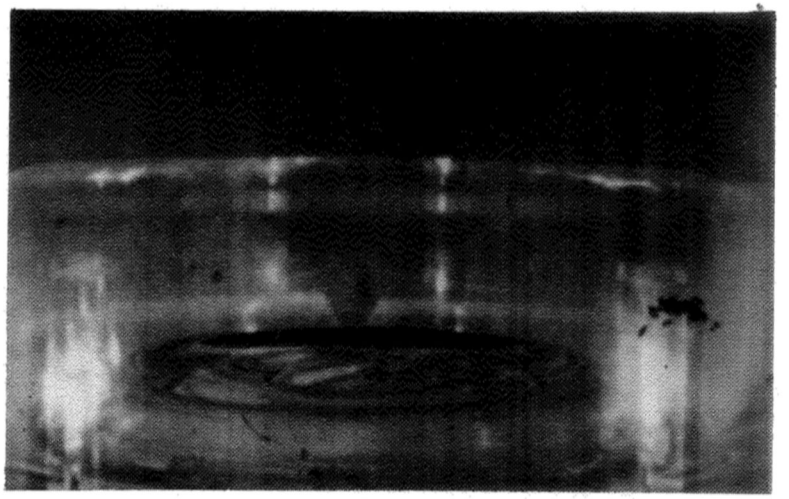


(d) 2.16 sec

Fig. I-24 2.3-, 4.7-, 13.2-, and 15.2-cm Cylinders at 0.016 g (Freon TF)



(a) 0.54 sec



(b) 1.08 sec



(c) 1.62 sec



(d) 2.16 sec

Fig. I-25 29.2-cm Cylinder at 0.016 g (Freon TF)

At 2.11 sec (Fig. I-23d), the interface has reached the bottom of the smaller vessel. Considerable turbulence is present at the top of the tank, along with some flow down the left side and interference ripples where this downward flow meets the upward-moving layer along the wall. In the larger tank, the remainder of the column formed as the result of Taylor instability is seen in the upper left corner. The top of the column has rebounded from the tank top. The bulk of the liquid is beginning to flow up the left side of the tank, following the Taylor instability.

In Fig. I-24, the test specimen consists of four cylinders whose inside diameters are 2.3, 4.7, 13.2, and 15.2 cm. Bond numbers immediately following capsule release are consequently 1.8, 7.6, 60, and 80.

At 0.27 sec (Fig. I-24a), a dome has formed in the 4.7-cm cylinder and is already beginning to recede. Flow features are just beginning to form in the two larger cylinders.

At 0.77 sec (Fig. I-24b), the dome in the 4.7-cm cylinder has receded into the downward-flowing liquid below. Broad domes have formed in the two larger cylinders; particular attention is called to the 13.2-cm cylinder, where the dome has a rather broad, flat upper surface on which a small depression can be seen.

At 0.98 sec, the depression mentioned immediately above has turned inside out, becoming a small, rapidly-growing proturberance on the top surface of the dome. Most of the liquid flow is now moving into this proturberance.

At 2.16 sec, the flow in the two larger cylinders is dominated by columns that have formed for the entire length of each cylinder. Very turbulent liquid, mixed with considerable gas, is collecting at the top of each of these cylinders. Liquid has also collected at the top of each of the smaller cylinders. In the 4.7-cm cylinder, considerable liquid that had collected at the top of the cylinder has splashed back down as a single coherent ball, seen moving down near the center of the cylinder.

Figure I-25 shows the largest test cylinder used -- 29.2 cm. Bond number is 280. Still photos probably do not show as convincingly as the motion picture that the entire length of the cylinder of liquid becomes hollow by the end of the test. It was found that motion picture projection was extremely helpful in the analysis of all of the flows of subregime 5E, whereas flows at lower Bond numbers could be studied more advantageously frame by frame.

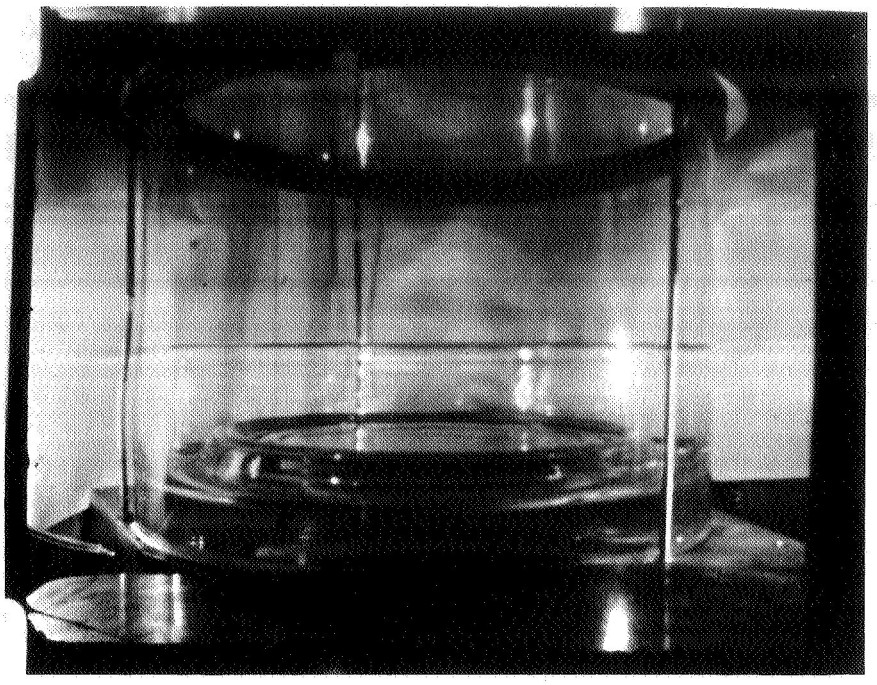
2. Extension to the Range of Settling Bond Numbers from 400 to 2000

A later experimental program was undertaken to extend the range of settling Bond numbers studied to greater magnitudes. Experiments were again performed in Martin-Denver's 75-ft drop tower, with the experiment package accelerated downward, relative to free fall, by an arrangement similar to that diagramed in Fig. I-20. In the new program, photographic techniques were modifed to allow a 44.5-cm-diameter test cylinder to be used, as shown in Fig. I-26. A larger outer capsule allowed accelerations as high as 0.042 g to be applied to the experiment package for the duration of the drop. Bond numbers from 460 to 1730 were investigated, using Freon TF (with a minute amount of dye) as the test liquid. Experimental procedure was essentially the same as that detailed in the preceding section, and data were again photographed at 200 frames per second.

Figures I-27 and I-28 show representative results. In general, the results were in good qualitative agreement with the theoretical predictions of the analytical sections above, in spite of the fact that contact angle was nearly zero, rather than nearly 90 deg as the linearization requires. Single, hollow liquid cylinders, of a larger diameter relative to the container diameter than was observed at lower Bond numbers, formed in all of the tests and grew toward the tops of the test vessels. Growth rates increased with increasing container acceleration.

The preceding subsection commented on an acceleration decrease with time following capsule release. This decrease was found to be due to inadequate clearance between the experiment package and the outer capsule used in that program. A device to calibrate the springs at various high rates of extension was constructed; it was found that the force delivered by the springs is, in general, nearly constant. Use of the larger outer capsule in this later program resulted in uniform and predictable experiment accelerations (as measured by various means) throughout the drop duration. Several of the earlier experiments were repeated with the new system; little change in basic liquid behavior was observed.

Fig. I-26 18-in. Test Specimen



(a) 1.0 sec



(b) 2.0 sec

Fig. I-27 B_R = -1200

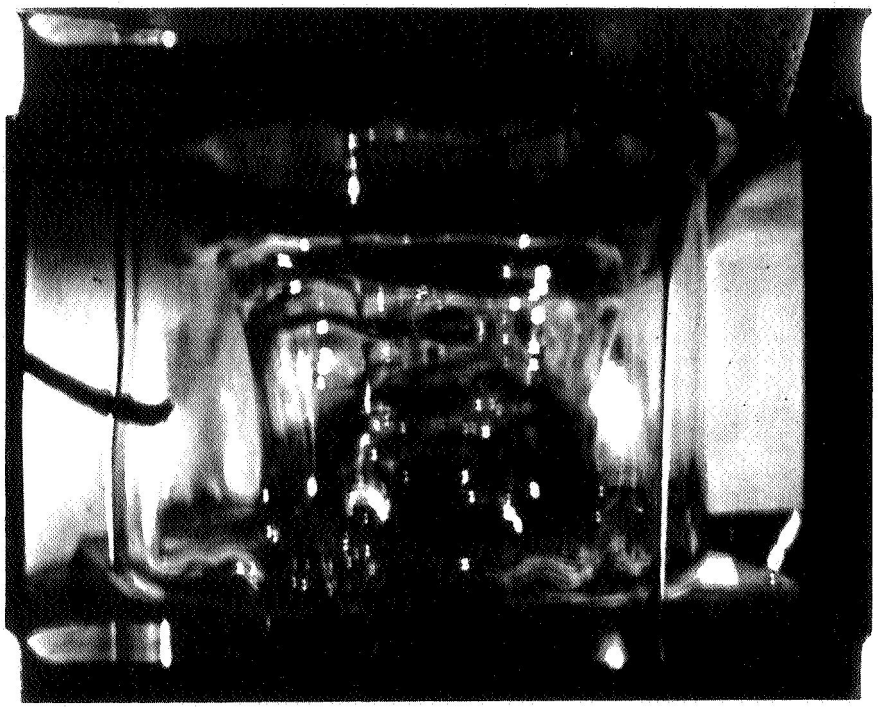


Fig. I-28 B_R = -1700 (1.5 sec)

The results of this and the preceding subsection show, as did the analysis, that primary aspects of the settling flow (not including velocities or rates of wave formation) can be validly scaled using Bond number, at least within the range covered by this portion of the investigation. Liquid level in the test vessel was not found to have an effect on the initial settling flow. Such secondary flow characteristics as viscous effects are of course not scaled by the Bond number. However, except for the tendency of a liquid spike to move to one side of the tank as a result of misalignment between the tank axis and the accelerations, these secondary flow features are of limited importance in understanding the basic nature of the flow. Velocities, which were not a primary consideration in this investigation, cannot be scaled (except perhaps in very special circumstances) without taking account, in the scale factor, of viscous effects, in addition to the other influences considered here.

It should be noted that the understanding of liquid settling gained in the course of this experimental investigation applies to the flow only up to the time when it reaches the aft end of the tank. After liquid has reached the aft end of the tank, its motion generally becomes quite turbulent, with liquid and gas phases becoming rather well mixed. Interference occurs between this fluid and the liquid that has not yet reached the aft end of the tank. In some cases, quantities of liquid are seen to splash back to the forward portion of the tank. Even if sufficient time were available to study this later phase of settling to any extent, it is doubtful that any means of scaling the experimental results to a full-scale vehicle tank could be found. The data would probably be of a statistical nature at best.

As a part of this second portion of the experimental investigation, a series of experiments were also run in which the test vessels were evacuated to approximately Freon saturation conditions before being dropped, and held at saturation conditions until actual capsule release, using the apparatus described in Volume II. No differences were observed between the settling of a saturated liquid and the settling of liquid at ambient conditions, which was studied in the main portions of the experimental program.

3. Investigation of the Effect of Offaxis Accelerations

A third experimental program was undertaken to investigate the problem of offaxis accelerations. As in the two previously described programs, experiments were performed in Martin-Denver's 75-ft drop tower, with the experimental package accelerated downward, relative to free fall, by an arrangement similar to that diagramed in Fig. I-20. The larger outer capsule mentioned in the preceding subsection was used; thus the accelerations applied to the experiments were found to be reasonably constant throughout each test. Experimental procedure was essentially the same as that detailed in the preceding subsections.

Test vessels were 15.2-cm inside diameter plexiglass cylinders. Their ends were milled at 1- and 10-deg angles to their axes, allowing them to be positioned rather accurately at those angles. The package as a whole was balanced before each test to ensure that the platform beneath the test vessels would be horizontal both before and during the test. Consequently, the cases, $\alpha_o = \alpha = 1$ deg and $\alpha_o = \alpha = 10$ deg, were investigated for various settling Bond numbers.

An early configuration of the experimental apparatus is shown in Fig. I-29, where the 200-frame-per-second motion picture camera is looking directly at a 10-deg specimen. The camera was later turned to the side to look at a front-surface mirror and thence at the specimen so that a larger field of view could be obtained. Test liquid was Freon TF (trichlorotrifluoroethane) in all the experiments. Contact angles were consequently near zero, as in the previously described experiments.

Photographs enlarged from the motion picture records of two of the experiments are shown in Fig. I-30. Acceleration was 0.015 g in each of these drops, giving a settling Bond number of 72. Aside from the angular behavior, development of the flow as a central spike and a layer on the wall is essentially the same as that observed at this settling Bond number in the axisymmetric investigation of the first experimental section above.

In the 1-deg cylinder, the liquid moves strongly to the right side, taking the base of the spike with it. The spike itself remains nearly vertical. In the 10-deg cylinder, on the other hand, bulk fluid motion is much less pronounced and is to the left side of the vessel.

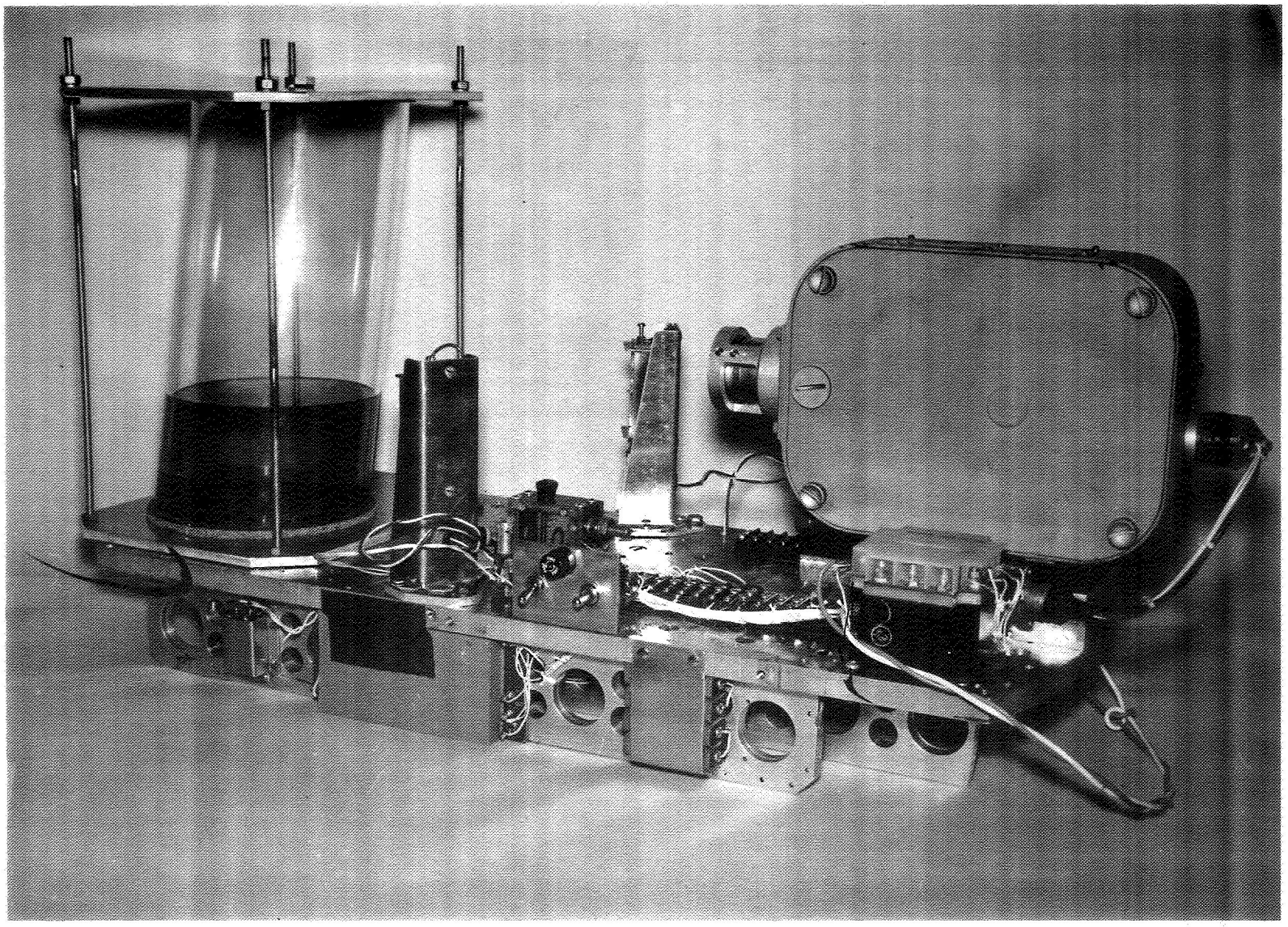
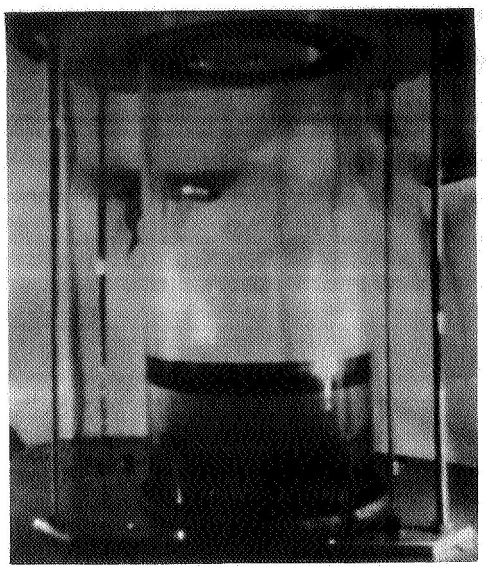
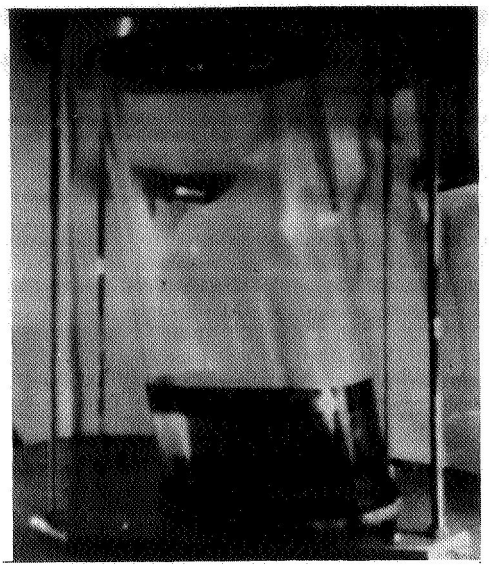


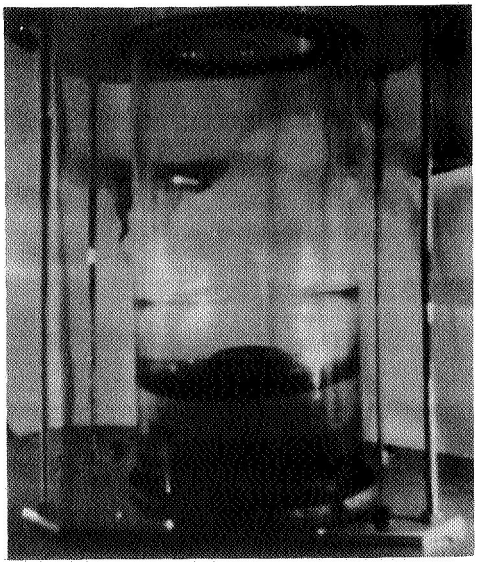
Fig. I-29 Experimental Apparatus



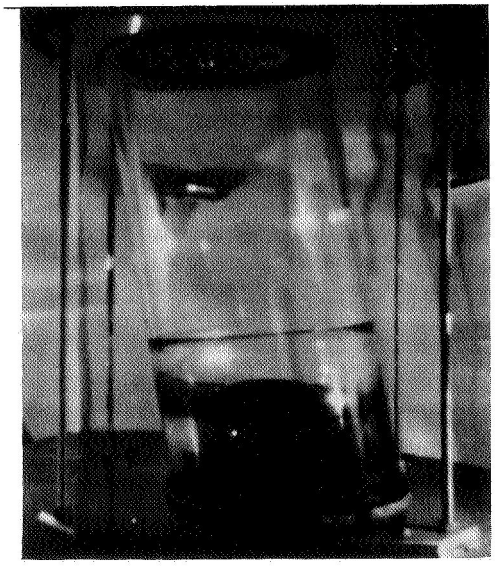
(a) t = 0.5 sec, $\alpha_o = \alpha$ = 1 deg



(b) t = 0.5 sec, $\alpha_o = \alpha$ = 10 deg

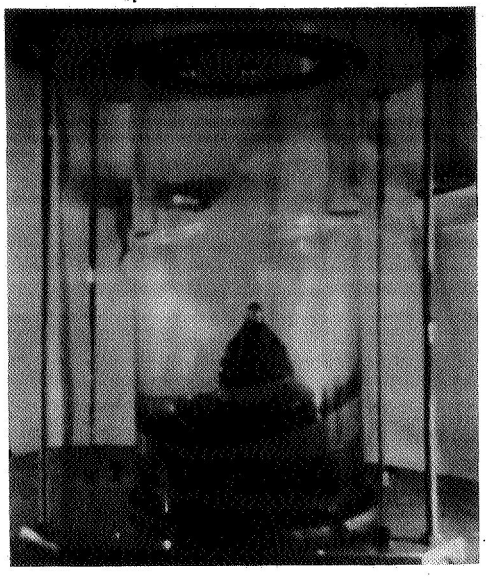


(c) t = 1.0 sec, $\alpha_o = \alpha$ = 1 deg

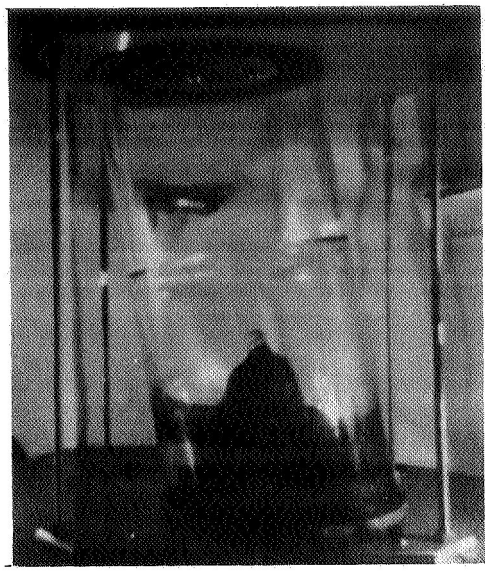


(d) t = 1.0 sec, $\alpha_o = \alpha$ = 10 deg

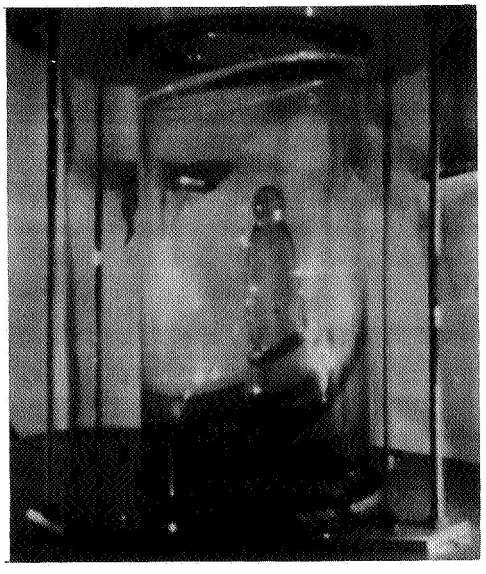
Fig. I-30 Experimental Results



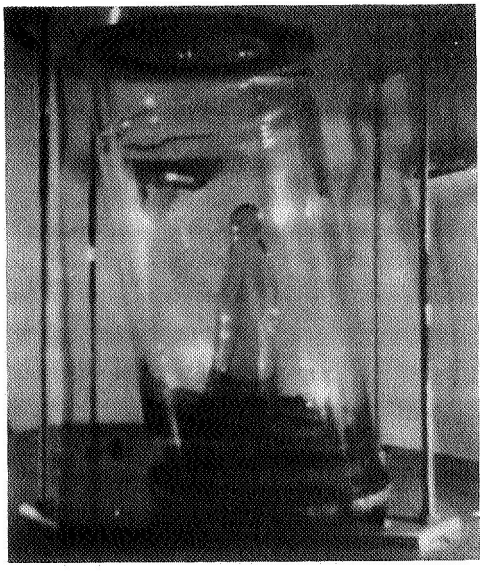
(e) t = 1.5 sec, $\alpha_o = \alpha$ = 1 deg



(f) t = 1.5 sec, $\alpha_o = \alpha$ = 10 deg



(g) t = 2.0 sec, $\alpha_o = \alpha$ = 1 deg



(h) t = 2.0 sec, $\alpha_o = \alpha$ = 10 deg

Fig. I-30 (concl)

The experiments were not as repeatable as most other experiments with vertical cylinders have been. While little difficulty in this respect was experienced with the 10-deg cylinder, a number of experiments with the 1-deg cylinder did not exhibit as pronounced a shift of the liquid to the side of the cylinder as shown in Fig. I-30. (There was always some shift, and always to the same side.) The series in Fig. I-30 was selected as being indicative of the behavior observed in most of the experiments, and also in a great many earlier vertical cylinder experiments, in which the cylinder could not be aligned very precisely.

Several experiments were also performed using a vertical cylinder of the same overall configuration as the 1- and 10-deg cylinders. Completely axisymmetric flow was never observed, although the surface did not generally tip a great deal and the spike stayed near the center. Such a shift as seen in Fig. I-30 was never observed in the vertical cylinder.

On the basis of these and the earlier experiments, it seems that the Bond number regime observed in this series (characterized by a dome forming in the center and becoming a thin spike) is particularly sensitive to slight deviations of the applied acceleration from an axial direction. While the degree to which asymmetric flow is observed within a 2-sec experiment duration is somewhat variable for slightly offaxis accelerations, the difficulty of obtaining axisymmetric flow experimentally indicates that it is unlikely that such flow could be depended on in an actual vehicle in this Bond number regime.

This aspect of the results is of considerable engineering significance. Both the analysis and, particularly, the experiments demonstrate that even a very slight misalignment of the acceleration, relative to the container axis, can result in liquid flow up one side of the container, rather than an axisymmetric flow coming together at the top. Figure I-31, which is similar to Fig. I-30g except that it was made with a 35-mm still camera some time after completion of the rest of the experimental program, is included to emphasize this result. Had it been possible to continue the experiment for a few more seconds, it seems certain that most of the liquid would have eventually gone up the right side, across the top, and back down the left side. Thus 1 deg of misalignment results, in this case, in establishment of flow that, because of its togetherness, does not soon lose its kinetic energy in collisions, or splashing, in a smooth-walled vessel, and consequently does not soon come to rest in the desired end of the vessel.

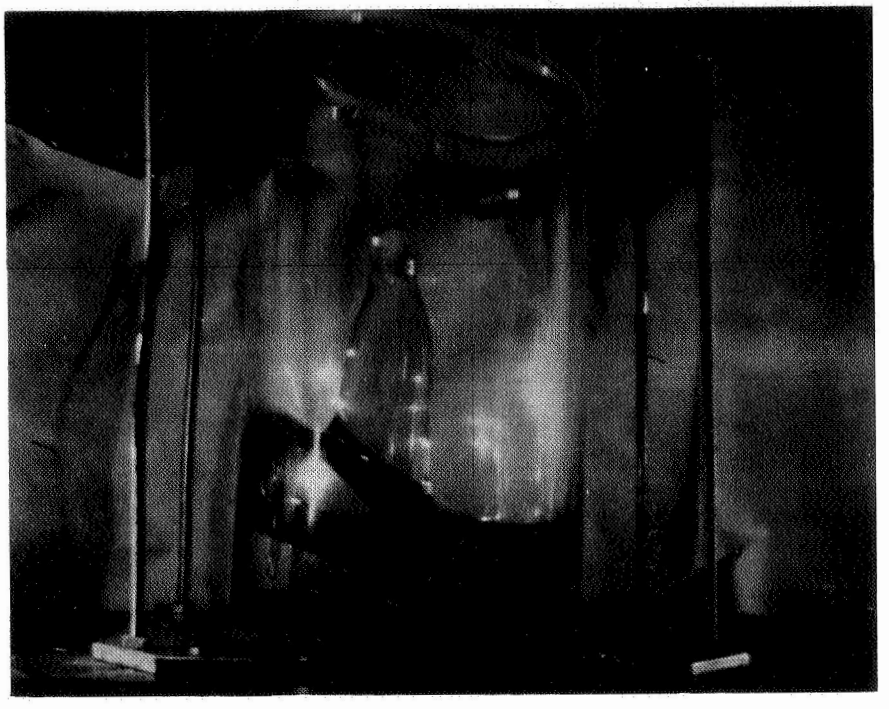


Fig. I-31 Influence of 1-deg Acceleration Misalignment on the Flow

The variability of the results obtained with nearly vertical cylinders indicates that the axisymmetric case is indeed singular. The surface response can become strongly asymmetric. The rate at which the asymmetries develop is somewhat unpredictable. For accelerations at greater angles to the axis, the surface response is again more predictable. In general, it is rather symmetric with respect to the direction of acceleration instead of the axis of the cylinder in these cases. Only when the two come close to coinciding is particularly radical behavior observed.

D. DISCUSSION AND CONCLUSIONS

1. Approximations in the Analysis

Weaknesses in the analysis result primarily from the linearization of the equations about a plane. As a result of this linearization, the analysis is strongest in those cases for which experiments were performed -- settling from an initially flat surface. The linearization is much more limiting in the three-dimensional case than in the axisymmetric case, moreover, in that it prohibits investigation of the importance of the θ-dependent terms in the solution relative to the axisymmetric portion.

If the equations were linearized about the actual initial liquid surface, the validity of the predictions for settling from curved surfaces could be checked. Although agreement with experiments was shown in those cases where experiments have been performed, the range of experiments performed with curved initial interfaces has been too limited for the agreement to be very conclusive.

The best analysis, of course, would not depend on any linearizations at all. Besides allowing study of the long-term growth of instabilities into flow features, such an analysis is also necessary before the behavior of a surface approaching the bottom of a tank can be studied, since linearization about any initial surface shape has the effect of letting the calculated surface profiles pass below the container bottom. Another advantage of a more exact analysis is that it would probably be able to accept initial surface motion. It might also be possible to include considerations of viscous effects, to some extent, in an exact analysis.

The linearized analysis does give a strong indication that more exact analyses would also fall short of being completely satisfactory due to an inability to adequately take account of contact angle dependence on fluid motion. The limitations of the linearized solution are manifest chiefly in the nature of the solution's dependence on contact angle, as was also true in the axisymmetric case. Because existing limitations to our understanding of contact angles are much more fundamental than the limitations of the analysis, it would seem that such refinements of the analysis as use of a numerical approach to allow linearization about an actual initial surface will continue to be limited until more knowledge of the dynamic behavior of contact angles is obtained.

2. Contact Angle

There are a number of interesting aspects of the manner in which the analytical solution depends on contact angle, in addition to the limitations mentioned in the preceding subsection. It should be noticed that contact angle limitations are manifest primarily when the analysis attempts to take account of offaxis accelerations. The axisymmetric portion of the solution does not show any qualitative variation in surface behavior with contact angle, although the scale of the response at any given time or, alternatively, the rate at which the perturbations grow depends on contact angle.

A further strong indication that the nature of the surface response, in the axisymmetric case, does not depend on contact angle is that the analytical results show good qualitative agreement with experimental results obtained with near-zero contact angles, even though such small contact angles plainly violate the restrictions imposed by the linearizations.

The reason for this lack of dependence on contact angle is that the contact angle constitutes a wall effect that is basically just a driving mechanism for the eventual surface response. The liquid surface right at the wall is either higher or lower than the surface away from the wall; consequently, the wall itself is the source of the perturbation that initiates the surface response. Thus the exact nature of the wall effect is not of great importance in determining the nature of the surface response, except perhaps for the surface response very near the wall.

The wall effect might have some influence on the rate of flow formation, however, as indicated by the dependence of the axisymmetric solution on contact angle. In particular, as the wall effect approaches zero, the time required for the surface displacement to reach any given amplitude approaches infinity. In this case, it is likely that in actuality the surface response would be driven by such extraneous perturbations as wall vibrations or residual fluid motion before the nearly-zero wall effect would have an influence. The eventual nature of the flow should still be similar to that studied, even though the development of the flow would proceed in an undetermined manner from a different type of source. The flow would likely be offaxis, since the perturbations providing its source would probably not be axisymmetric. It should be remembered that the wall effect approaches zero only when $\gamma \rightarrow 90$ deg, $\alpha_o \rightarrow 0$, and $\alpha \rightarrow 0$ simultaneously, as discussed in the analytical section that dealt with offaxis accelerations.

3. Conclusions

Because of the analytical limitations discussed above, present understanding of the response of contained liquids to acceleration reversals must still be based primarily on experimental results. The analysis is a valuable aid to understanding the experimental results, however. In addition, it gives a basis for predicting flow behavior in cases that have not been experimentally investigated, e.g., low gravity initial conditions and nonwetting liquids. Comparison of theory and experiment in cases where both are available gives some basis for extrapolation in other cases.

The practical value of the analysis is largely based on the fact that it gives good qualitative agreement with experimental results in cases where experiments have been performed. Quantitative agreement is not possible since the axisymmetric portion of the analysis gives displacements and velocities proportional to ctn γ, which blow up as γ approaches zero.

The experimental results provide a valid representation of what would occur in an actual space vehicle tank for the same initial conditions and boundary conditions. Both the analysis and the experiments show that primary aspects of the settling flow are scaled by Bond number. The analysis further shows that these same flow characteristics should be essentially independent of contact angle.

Both the analysis and the experiments also showed that the axisymmetric case is in some ways singular. Accelerations that are very slightly offaxis can result in almost all of the liquid moving up one side of the container.

Engineering questions relating to flow velocities and the total amount of time required for liquid to move from one end of a tank to the other and come to rest again still cannot be answered. Drop tower experiments have not been able to adequately investigate these long duration effects. The analysis does not really even consider flow characteristics, much less the fluid behavior once the flow has reached the end of the tank, and also does not take into account the effects of viscosity and contact angle variations, both of which are important in considering flow velocities.

II. RECOMMENDATIONS

Since it is felt by the authors that a point of diminishing returns has been reached in both drop-tower investigations and analyses of fluid phenomena of the type described in this report, it is recommended that attention in the future be turned to research performed in space, where a whole new realm of long-duration experiments could be performed.

In particular, manned scientific experiments in space will be an extremely valuable means of investigating the long-term response of liquids to acceleration changes. The ability to perform manned orbiting experiments will be a tremendous step forward in that a scientist-astronaut could, for instance, control the experiments on the basis of direct observation, make photographic and optical adjustments as needed, reload cameras, and plan new experiments on the basis of the outcome of just-completed experiments.

One type of study that might be fruitfully pursued in the immediate future, in addition to orbiting experiments, is the area of nonlinear analyses of propellant tank hydrodynamics. It seems quite probable that numerical techniques can be used to obtain a more sophisticated theoretical understanding of the response of contained liquids to changing accelerations.

Another area in which significant advances might be made, without going to orbiting experiments, is the study of contact angles. The analysis of liquid surface dynamics presented in this report, as well as most other such published analyses, assumed uniform, constant contact angles. The only analyses that are not postulated on this type of contact angle behavior make equally simple assumptions. Although it is known that contact angles are somewhat affected by relative velocities between fluids and solid walls, the nature of this variation is not understood. Thus a major shortcoming of the analysis will probably not be rectified until more basic knowledge of contact angle is obtained. Although the basic scientific research necessary to gain that knowledge was obviously beyond the scope of this investigation, it does seem that such drop towers as the one used for the experimental portion have now been developed to a level of sophistication where they could fruitfully be used to investigate some basic contact phenomena problems.

III. REFERENCES

1. F. Bashforth and J. C. Adams: An Attempt to Test the Theories of Capillary Action. Cambridge University Press, England, 1883.

2. S. Fordham: "On the Calculation of Surface Tension from Measurements of Pendant Drops." Proceedings of the Royal Society, A, Vol 194, 1948, p 1 thru 16.

3. D. N. Staicopolus: "The Calculation of Surface Tension and of Contact Angle by the Sessile-Drop Method." Journal of the Colloid Sciences, Vol 17, 1962, p 439 thru 447, and Vol 18, 1963, p 793 and 794.

4. H. M. Satterlee and J. H. Chin: "Menicus Shape under Reduced Gravity Conditions." Fluid Mechanics and Heat Transfer under Low Gravity. H. Cohan and M. Rogers (ed), USAF Office of Scientific Research and Lockheed Missiles and Space Co., June 1965, p 13-1 thru 13-24.

5. W. H. Jurney: The Configuration of a Contained Liquid in a Constant Gravitational Field. TM-0444-65-4. Martin Company, Denver, Colorado, October 1965.

6. T. E. Bowman, B. K. Larkin, and J. L. McGrew: Phase I Report, Criteria for Cryogenic Liquid Experiments in Orbit. CR-65-24, Martin Company, Denver, Colorado, October 1965.

7. B. K. Larkin: "Numerical Solution of the Equation of Capillarity." Journal of the Colloid Sciences. (To be published)

8. G. B. Airy: "Tides and Waves," in Encyclopedia Metropolitana. Vol V, 1845, p 281 thru 344.

9. G. G. Stokes: "On the Theory of Oscillatory Waves." Cambridge Transactions 8, 1847, p 441 thru 455.

10. W. Thomson (Lord Kelvin): "Hydrokinetic Solutions and Observations." Phil. Mag. Series IV, 42, 1871, p 362 thru 377.

11. J. C. Maxwell: "Capillary Action." Encyclopedia Britannica, 9th ed. 1878; also ibid: Scientific Papers, 2, Cambridge, 1890, p 541 thru 591.

12. P. Concus: "Capillary Stability in an Inverted Rectangular Tank." Advances in the Astronautical Sciences, 14, 1963, p 21 thru 37.

13. H. M. Satterlee and W. C. Reynolds: The Dynamics of the Free Liquid Surface in Cylindrical Containers under Strong Capillary and Weak Gravity Conditions. Technical Report LG-2, Stanford University, May 1964.

14. R. E. Moore and L. M. Perko: "Inviscid Fluid Flow in an Accelerating Cylindrical Container." Journal of Fluid Mechanics, 22, 1965, p 305 thru 320.

15. P. Concus, G. E. Crane, and L. M. Perko: "Inviscid Fluid Flow in an Accelerating Axisymmetric Container." pp 3-1 to 3-20 in Fluid Mechanics, op cit.

16. F. C. W. Fung: "Dynamic Response of Liquids in Partially Filled Containers Suddenly Experiencing Weightlessness." pp 7-1 to 7-32 in Fluid Mechanics, op cit.

17. W. J. Harrison: "The Influence of Viscosity on the Oscillations of Superposed Fluids." Proceedings of the London Mathematical Society, Series 2, Vol 6, 1908, p 396 thru 405.

18. R. Bellman and R. H. Pennington: "Effects of Surface Tension and Viscosity on Taylor Instability." Quarterly Journal of Applied Mathematics, Vol 12, 1954, p 151 thru 162.

19. S. Chandrasekhar: "The Character of the Equilibrium of an Incompressible Heavy Viscous Fluid of Variable Density." Proceedings of the Cambridge Philosophical Society, Vol 51, 1955, p 162 thru 178.

20. S. Chandrasekhar: Hydrodynamic and Hydromagnetic Stability. Chapter X. Clarendon Press, Oxford, 1961.

21. W. H. Reid: "The Effects of Surface Tension and Viscosity on the Stability of Two Superposed Fluids." Proceedings of the Cambridge Philosophical Society, Vol 57, 1961, p 415 thru 425.

22. A. J. Willson: "On the Stability of Two Superposed Fluids." Proceedings of the Cambridge Philosophical Society, Vol 61, 1965, p 595 thru 607.

23. D. J. Lewis: "The Instability of Liquid Surfaces when Accelerated in a Direction Perpendicular to Their Planes. II." Proceedings of the Royal Society, A, Vol 202, 1950, 81 thru 96. Also, J. Allred and G. Blount: Experimental Studies of Taylor Instability. LA-1600, Los Alamos Scientific Laboratory, Los Alamos, New Mexico, 1953.

24. H. W. Emmons, C. T. Chang, and B. C. Watson: "Taylor Instability of Finite Surface Waves." Journal of Fluid Mechanics, Vol 7, 1960, p 177 thru 193.

25. W. J. Masica and D. A. Petrash: Motion of Liquid-Vapor Interface in Response to Imposed Acceleration. NASA TN D-3005, September 1965. Also, W. J. Masica and J. A. Salzman: "An Experimental Investigation of the Dynamic Behavior of the Liquid-Vapor Interface under Adverse Low-Gravitational Conditions." p 2-1 thru 2-18 in Fluid Mechanics, op cit.

26. M. P. Hollister and H. M. Satterlee: "Low Gravity Liquid Reorientation." p 8-1 thru 8-32 in Fluid Mechanics, op cit.

27. T. E. Bowman: "Liquid Settling in Large Tanks." p 14-1 thru 14-21 in Fluid Mechanics, op cit.

28. T. E. Bowman: "Dynamics of an Axisymmetric Liquid Free Surface following a Stepwise Acceleration Change." 1966 Proceedings, Institute of Environmental Sciences, April 1966, p 553 thru 560.

29. T. E. Bowman: "Response of the Free Surface of Cylindrically Contained Liquid to Off-Axis Accelerations." Proceedings of the 1966 Heat Transfer and Fluid Mechanics Institute, ed. M. A. Saad and J. A. Miller, Stanford University Press, 1966, p 295 thru 314.

30. F. P. Bretherton: "The Motion of Long Bubbles in Tubes." Journal of Fluid Mechanics, Vol 10, 1961, p 166 thru 188.

31. D. F. Gluck and J. P. Gille: "Fluid Mechanics of Zero-g Propellant Transfer in Spacecraft Propulsion Systems." Trans. ASME, Vol 87B, 1965, p 1 thru 8.

32. S. Hattori: On the Motion of a Cylindrical Bubble in a Tube and Its Application to the Measurement of the Surface Tension of a Liquid. Report 115, Aeronautical Research Institute, Tokyo Imperial University, Tokyo, 1935.

33. W. J. Masica, D. A. Petrash, and E. W. Otto: Hydrostatic Stability of the Liquid-Vapor Interface in a Gravitational Field. NASA TN D-2267, May 1964.

34. W. J. Masica, J. D. Derdul, and D. A. Petrash: Hydrostatic Stability of the Liquid-Vapor Interface in a Low-Acceleration Field. NASA TN D-2444, August 1964.

35. H. L. Paynter: "The Martin Company's Low-g Experimental Facility." p 15-1 thru 15-17 in Fluid Mechanics, op cit.

NASA-Langley, 1966

"The aeronautical and space activities of the United States shall be conducted so as to contribute . . . to the expansion of human knowledge of phenomena in the atmosphere and space. The Administration shall provide for the widest practicable and appropriate dissemination of information concerning its activities and the results thereof."

—NATIONAL AERONAUTICS AND SPACE ACT OF 1958

NASA SCIENTIFIC AND TECHNICAL PUBLICATIONS

TECHNICAL REPORTS: Scientific and technical information considered important, complete, and a lasting contribution to existing knowledge.

TECHNICAL NOTES: Information less broad in scope but nevertheless of importance as a contribution to existing knowledge.

TECHNICAL MEMORANDUMS: Information receiving limited distribution because of preliminary data, security classification, or other reasons.

CONTRACTOR REPORTS: Technical information generated in connection with a NASA contract or grant and released under NASA auspices.

TECHNICAL TRANSLATIONS: Information published in a foreign language considered to merit NASA distribution in English.

TECHNICAL REPRINTS: Information derived from NASA activities and initially published in the form of journal articles.

SPECIAL PUBLICATIONS: Information derived from or of value to NASA activities but not necessarily reporting the results of individual NASA-programmed scientific efforts. Publications include conference proceedings, monographs, data compilations, handbooks, sourcebooks, and special bibliographies.

Details on the availability of these publications may be obtained from:

SCIENTIFIC AND TECHNICAL INFORMATION DIVISION

NATIONAL AERONAUTICS AND SPACE ADMINISTRATION

Washington, D.C. 20546